

# Convex Optimization of Distributed Cooperative Detection in Multi-Receiver Molecular Communication

Yuting Fang, *Student Member, IEEE*, Adam Noel, *Member, IEEE*, Nan Yang, *Member, IEEE*,  
Andrew W. Eckford, *Senior Member, IEEE*, and Rodney A. Kennedy, *Fellow, IEEE*

**Abstract**—In this paper, the error performance achieved by cooperative detection among  $K$  distributed receivers in a diffusion-based molecular communication (MC) system is analyzed and optimized. In this system, the receivers first make local hard decisions on the transmitted symbol and then report these decisions to a fusion center (FC). The FC combines the local hard decisions to make a global decision using an  $N$ -out-of- $K$  fusion rule. Two reporting scenarios, namely, perfect reporting and noisy reporting, are considered. Closed-form expressions are derived for the expected global error probability of the system for both reporting scenarios. New approximated expressions are also derived for the expected error probability. Convex constraints are then found to make the approximated expressions jointly convex with respect to the decision thresholds at the receivers and the FC. Based on such constraints, suboptimal convex optimization problems are formulated and solved to determine the optimal decision thresholds which minimize the expected error probability of the system. Numerical and simulation results reveal that the system error performance is greatly improved by combining the detection information of distributed receivers. They also reveal that the solutions to the formulated suboptimal convex optimization problems achieve near-optimal global error performance.

**Index Terms**—Molecular communication, multi-receiver cooperation, error performance, convex optimization.

## I. INTRODUCTION

OVER the past decades there have been considerable advancements in the fields of nanotechnology and biological science, where the design and manufacturing of nanoscale ( $< 0.1\mu\text{m}$ ) and microscale ( $0.1 - 100\mu\text{m}$ ) devices, referred to as nanomachines, have begun to take shape [2]. Since nanomachines are only capable of performing simple computing, data storing, sensing, and actuation tasks, it is envisioned that they can be interconnected to execute more elaborate and challenging tasks in a collaborative and distributed manner. The resulting network, i.e., nanonetwork, is anticipated to expand the capabilities of single nanomachines by allowing them to exchange information and interact with each other. Looking 10–20 years ahead, nanonetworks will advance a

diverse number of potential applications, such as disease detection, targeted drug delivery, and pollution control [3].

Molecular communication (MC) has been acknowledged as one of the most promising nanoscale communication paradigms in bio-inspired nanonetworks, due to its unique potential benefits of bio-compatibility and low energy consumption [4]. In fact, MC is present in nature and used by biological entities and systems, such as molecules, cells, and microorganisms. In MC, a transmitter releases tiny particles such as molecules or lipid vesicles into a fluid medium, where the particles propagate until they arrive at a receiver. The receiver then detects the information encoded in these particles [5]. The simplest molecular propagation mechanism is free diffusion where the information-carrying particles propagate from the transmitter to the receiver via Brownian motion. The transmitter does not need to expend any energy to use this mechanism.

One of the primary challenges posed by diffusion-based MC is that its reliability rapidly decreases when the transmitter-receiver distance increases. One approach to enhancing its reliability is to use multiple receivers sharing common information to help transmission. In biological environments, some cells or organisms indeed share common information to achieve a specific task [6], e.g., calcium ( $\text{Ca}^{2+}$ ) signaling [7]. In one process regulated by  $\text{Ca}^{2+}$  signaling, named excitation-contraction coupling, the cells in skeletal muscle share  $\text{Ca}^{2+}$  ions to induce the contraction of myofibrils [8].

The majority of the existing MC studies have focused on the modeling of a single-receiver MC system. Recent studies, e.g., [9–16], have expanded the single-receiver MC system to the multi-receiver MC system. For example, [9, 10] analyzed the transmission rate of the molecular broadcast system where a single transmitter transmits molecular information to multiple receivers. In [11], simulations were performed to demonstrate the feasibility of a bio-nanosensor network where bacteria-based bio-nanomachines collectively perform target detection and tracking. In [12], the communication process between two populations of bacteria through a diffusion channel was studied. In [13], the microfluidic channel with two transmitter and receiver pairs was explored. Focusing on the communication between a group of transmitters and a group of receivers, [14] optimized the transmission rate at each transmitter. A new stochastic model was proposed in [15] to model the MC system with multiple transmitters and receivers. Recently, [16] designed a multiple-input multiple-output MC system and characterized the inter-symbol and

This work was presented in part at the IEEE GLOBECOM 2016 [1].

Y. Fang, N. Yang, and R. A. Kennedy are with the Research School of Engineering, The Australian National University, Canberra, ACT 2601, Australia (e-mail: {yuting.fang, nan.yang, rodney.kennedy}@anu.edu.au).

A. Noel is with the School of Electrical Engineering and Computer Science, University of Ottawa, Ottawa, ON K1N 6N5, Canada (e-mail: anoel2@uottawa.ca).

A. W. Eckford is with the Department of Electrical Engineering and Computer Science, York University, Toronto, ON M3J 1P3, Canada (e-mail: aeckford@yorku.ca)

inter-link interference therein. While [9–16] stand on their own merits, the role of the *cooperation* among multiple receivers in determining the transmitter’s intended symbol sequence in a multi-receiver MC system has not been established in the literature.

We note that the cooperation among distributed detectors in wireless communications has been identified as an effective means of improving performance. For example, cooperative spectrum sensing is achieved by allowing multiple secondary users to share sensing data to improve the detection quality of a primary user [17]. Generally, in a distributed detection system the data of the individual detectors is shared at a fusion center (FC). This data may be hard (binary) decisions, soft (multi-level) decisions, or quantized observations. The FC then appropriately combines the received data to yield a global inference [18] using a fusion rule, such as the AND rule and OR rule for hard decisions. In fact, logic operations and corresponding computations required at the FC, e.g., AND, OR, and addition operations, can be implemented at the molecular level [19, 20]. Therefore, MC is a suitable domain to apply distributed detection to improve transmission reliability. We note that this application has not been previously studied.

In this paper, we for the first time quantify and maximize the benefits of multi-receiver cooperation in a cooperative diffusion-based MC system. Our goal is to establish a fundamental understanding of the reliability improvement brought by combining the detection results of distributed receivers at an FC. In our considered system, for each symbol transmitted from the transmitter, the receivers first independently make local hard decisions on the transmitted symbol and then report their decisions to the FC. We note that the role of the receivers in our considered system appears similar to that of decode-and-forward (DF) relays in wireless systems [21]. However, the results for DF relaying cannot be used in the MC system, due to the fact that the characteristics of the propagation channel and the methods for recovering the received symbols in MC systems are completely different from those in wireless systems. After receiving the local hard decisions, the FC fuses all decisions to make a global decision on the transmitted symbol using an  $N$ -out-of- $K$  fusion rule. Here, we consider two different reporting scenarios from the receivers to the FC, namely, perfect reporting and noisy reporting. In this work, we assume that the FC does not feed back its global decision to receivers. We also assume that each receiver transmits a unique type of molecule and the FC is able to simultaneously and independently detect the different types of molecules from the receivers<sup>1</sup> (as in [6]). To maximize the benefits of multi-receiver cooperation in the system, we determine the jointly optimal decision thresholds at the receivers and the FC such that the expected global error probability is minimized. To achieve this minimization, we develop new convex analysis of the error performance for the system having a symmetric topology. In the symmetric topology, the distances between the transmitter and the receivers are identical and the distances be-

tween the receivers and the FC are also identical. This results in independent and *identically* distributed observations at the receivers. We clarify that the assumption of the symmetric topology is to improve the tractability of our convex analysis and this assumption will be relaxed in future work. We note that the expected error probability of a point-to-point MC link is minimized in [22], by deriving a closed-form analytical expression for the optimal decision threshold at the receiver. However, the derived optimal decision threshold in [22] cannot be applied or extended to the cooperative MC system.

The primary contributions of this paper, especially relative to our previous work [1], are summarized as follows:

- 1) We derive closed-form expressions for the expected global error probabilities of the cooperative MC system in the perfect and noisy reporting scenarios. We clarify that a symbol-by-symbol detection with a constant decision threshold at all receivers and the FC is considered in this derivation.
- 2) We derive new approximated expressions for the expected global error probability of the cooperative MC system in both reporting scenarios. We also derive additional convex constraints under which the approximated expressions are jointly convex with respect to the decision thresholds at the receivers and the FC.
- 3) Based on the derived convex approximations and constraints, we formulate suboptimal convex optimization problems for a given transmitted symbol sequence. For the sake of practicality, we then extend the formulated convex optimization problems such that a single optimal threshold is determined to minimize the average error performance over all realizations of transmitted symbol sequences.

Using numerical and simulation results, we demonstrate that the error performance of the cooperative MC system is much better than that of the point-to-point MC link. We also demonstrate the effectiveness of our formulated suboptimal convex optimization problems by showing that near-optimal global error performance is achieved by using the solutions to our formulated problems, i.e., the optimal thresholds. In this work, the optimality of the performance refers to the accuracy of the optimization to find the optimal thresholds in the symbol-by-symbol detection.

The rest of this paper is organized as follows. In Section II, we describe the system model. In Section III, we present the error performance analysis of the cooperative-receiver MC system. In Section IV, we formulate convex optimization problems of the cooperative-receiver MC system. Numerical and simulation results are provided in Section V. In Section VI, we conclude and describe future directions for this work.

## II. SYSTEM MODEL

In this paper we consider a cooperative MC system in a three-dimensional space, as depicted in Fig. 1, which consists of one transmitter (TX), a “cluster” of  $K$  receivers (RXs), and one device acting as an FC. the FC is not included in the set of RXs. We assume that all RXs and the FC are spherical observers. Accordingly, we denote  $V_{\text{RX}_k}$  and  $r_{\text{RX}_k}$  as the volume

<sup>1</sup>We note that releasing a unique type of molecule at each receiver may not be realistic in some cases. However, this assumption gives a lower bound on the error performance of the cooperative MC system using a hard decision fusion rule.

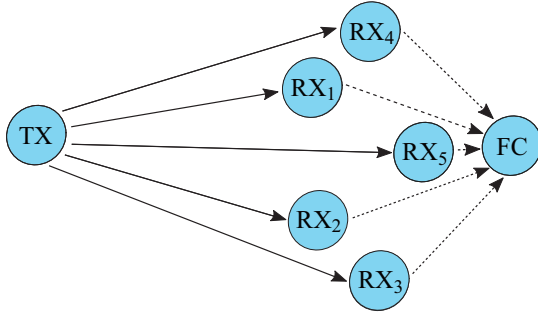


Fig. 1. An example of a cooperative MC system with  $K = 5$ , where the transmission from the TX to the RXs is represented by solid arrows and the decision reporting from the RXs to the FC is represented by dashed arrows.

and the radius of the  $k$ th RX,  $RX_k$ , respectively, where  $k \in \{1, 2, \dots, K\}$ . We also denote  $V_{FC}$  and  $r_{FC}$  as the volume and the radius of the FC, respectively. We also assume that the RXs and the FC are independent passive observers such that molecules can diffuse through them without reacting. We further assume that all individual observations are independent of each other. In addition, we assume that the RXs operate in the half-duplex mode such that they do not receive information and report their local decisions at the same time.

In the considered system, the transmission of each information symbol from the TX to the FC via RXs is completed within three phases, detailed as follows:

- In the first phase, the TX transmits one symbol of information via type  $A_0$  molecules to the RXs through the diffusive channel. The number of the released type  $A_0$  molecules is denoted by  $S_0$ . We assume that the diffusion of all individual molecules is independent. The type  $A_0$  molecules transmitted by the TX are detected by all RXs. In this work we consider that the TX uses ON/OFF keying [23] to convey information. As per the rules of ON/OFF keying, the TX releases  $S_0$  molecules of type  $A_0$  to convey information symbol “1”, and releases no molecules to convey information symbol “0”. To enable ON/OFF keying, the information transmitted by the TX is encoded into an  $L$ -length binary sequence, denoted by  $\mathbf{W}_{TX} = \{W_{TX}[1], W_{TX}[2], \dots, W_{TX}[L]\}$ , where  $W_{TX}[j]$ ,  $j \in \{1, \dots, L\}$ , is the  $j$ th symbol transmitted by the TX. We assume that the probability of transmitting “1” in the  $j$ th symbol is  $P_1$  and the probability of transmitting “0” in the  $j$ th symbol is  $1 - P_1$ , i.e.,  $\Pr(W_{TX}[j] = 1) = P_1$  and  $\Pr(W_{TX}[j] = 0) = 1 - P_1$ , where  $\Pr(\cdot)$  denotes probability.
- In the second phase, each RX makes a local hard decision on the current transmitted symbol. We denote  $\hat{W}_{RX_k}[j]$  as the local hard decision on the  $j$ th transmitted symbol at  $RX_k$ . Then, the RXs simultaneously report their local  $j$ th hard decisions to the FC. We assume that  $RX_k$  transmits type  $A_k$  molecules, which can be detected by the FC. The number of the released type  $A_k$  molecules is denoted by  $S_k$ . We also assume that the channel between each RX and the FC is diffusion-based, and each RX uses ON/OFF keying to report its local hard decision.
- In the third phase, the FC obtains the decision at  $RX_k$  by receiving type  $A_k$  molecules over the  $RX_k - FC$  link. We

assume that the  $K$   $RX_k - FC$  links are independent. We denote  $\hat{W}_{FC_k}[j]$  as the received local decision of  $RX_k$  on the  $j$ th transmitted symbol at the FC. the FC combines all  $\hat{W}_{FC_k}[j]$  using an  $N$ -out-of- $K$  fusion rule to make a global decision  $\hat{W}_{FC}[j]$  on the  $j$ th symbol transmitted by the TX. As per the  $N$ -out-of- $K$  fusion rule, the FC declares a global decision of “1” when it receives at least  $N$  decisions of “1”. There are several special cases of the  $N$ -out-of- $K$  fusion rule, such as 1) majority rule where  $N = \lceil K/2 \rceil$  and  $\lceil x \rceil$  represents the smallest integer greater than or equal to  $x$ , 2) OR rule where  $N = 1$ , and 3) AND rule where  $N = K$ .

We define  $\mathbf{W}_{TX}^l = \{W_{TX}[1], \dots, W_{TX}[l]\}$  as an  $l$ -length subsequence of the information transmitted by the TX, where  $l \leq L$ . We also define  $\hat{\mathbf{W}}_{RX_k}^l = \{\hat{W}_{RX_k}[1], \dots, \hat{W}_{RX_k}[l]\}$  as an  $l$ -length subsequence of the local hard decisions at  $RX_k$ . We then define  $\hat{\mathbf{W}}_{FC_k}^l = \{\hat{W}_{FC_k}[1], \dots, \hat{W}_{FC_k}[l]\}$  as an  $l$ -length subsequence of the received local decision of  $RX_k$  at the FC. We further define  $\hat{\mathbf{W}}_{FC}^l = \{\hat{W}_{FC}[1], \dots, \hat{W}_{FC}[l]\}$  as an  $l$ -length subsequence of the global decisions at the FC.

We denote  $t_{trans}$  as the transmission interval time from the TX to the RXs and  $t_{report}$  as the report interval time from the RXs to the FC. Thus, the symbol interval time from the TX to the FC is given by  $T = t_{trans} + t_{report}$ . At the beginning of the  $j$ th symbol interval, i.e.,  $(j-1)T$ , the TX transmits  $W_{TX}[j]$ . After this the TX keeps silent until the start of the  $(j+1)$ th symbol interval. We apply the weighted sum detector with equal weights [24] at the RXs and FC for detection. Thus, the RXs and FC each take multiple samples within their corresponding interval time, add the individual samples with equal weights, and compare the summation with a decision threshold. The decision thresholds at  $RX_k$  and FC are denoted by  $\xi_{RX_k}$  and  $\xi_{FC}$ , respectively. Here, the assumption of equal weights for all samples is adopted to limit the computational complexity of the detector and facilitate its usage in MC.

We now describe the sampling schedules of the RXs and FC. All RXs sample at the same times and take  $M_{RX}$  samples per symbol interval. The time of the  $m$ th sample for each RX in the  $j$ th symbol interval is given by  $t_{RX}(j, m) = (j-1)T + m\Delta t_{RX}$ , where  $\Delta t_{RX}$  is the time step between two successive samples at each RX,  $m \in \{1, 2, \dots, M_{RX}\}$ , and  $M_{RX}\Delta t_{RX} < t_{trans}$ . At the time  $(j-1)T + t_{trans}$ , each RX reports its local decision for the  $j$ th interval via diffusion to the FC. We assume that the FC takes  $M_{FC}$  samples of *each* type of molecule in every reporting interval. The time of the  $\tilde{m}$ th sample of type  $A_k$  molecules at the FC in the  $j$ th symbol interval is given by  $t_{FC}(j, \tilde{m}) = (j-1)T + t_{trans} + \tilde{m}\Delta t_{FC}$ , where  $\Delta t_{FC}$  is the time step between two successive samples at the FC and  $\tilde{m} \in \{1, 2, \dots, M_{FC}\}$ .

### III. ERROR PERFORMANCE ANALYSIS

In this section, we analyze the expected global error probability<sup>2</sup> of the cooperative MC system. To this end, we denote  $Q_{FC}[j]$  as the expected global error probability in the  $j$ th

<sup>2</sup>All the expected error probabilities throughout this paper are derived for given  $\mathbf{W}_{TX}^{j-1}$ , unless otherwise specified.

symbol interval for a *given* transmitter sequence  $\mathbf{W}_{\text{TX}}^{j-1}$ . Under the assumption that there is no *a priori* knowledge of  $W_{\text{TX}}[j]$ , we express  $Q_{\text{FC}}[j]$  as

$$Q_{\text{FC}}[j] = P_1 Q_{\text{md}}[j] + (1 - P_1) Q_{\text{fa}}[j], \quad (1)$$

where  $Q_{\text{md}}[j]$  denotes the expected global missed detection probability (MDP) in the  $j$ th symbol interval and  $Q_{\text{fa}}[j]$  denotes the expected global false alarm probability (FAP) in the  $j$ th symbol interval. By averaging  $Q_{\text{FC}}[j]$  over all possible realizations of  $\mathbf{W}_{\text{TX}}^{j-1}$  and across all symbol intervals, the expected average error probability of the cooperative MC system,  $\bar{Q}_{\text{FC}}$ , can be obtained. In the analysis, we address two different reporting scenarios, namely, perfect reporting and noisy reporting. In the perfect reporting scenario, we assume that no error occurs when  $\text{RX}_k$  reports to the FC, i.e.,  $\hat{W}_{\text{FC}}[j] = \hat{W}_{\text{RX}_k}[j]$ . In the noisy reporting scenario, errors can occur when  $\text{RX}_k$  reports to the FC via diffusion<sup>3</sup>.

#### A. Perfect Reporting

In this subsection, we start our analysis by examining the error performance of the TX –  $\text{RX}_k$  link. This examination is based on the analysis in [22]. We then use the results of this examination to analyze  $Q_{\text{md}}[j]$  and  $Q_{\text{fa}}[j]$  in the perfect reporting scenario to obtain  $Q_{\text{FC}}[j]$ .

1) TX –  $\text{RX}_k$  Link: We first evaluate the probability of observing a given type  $A_0$  molecule, emitted from the TX at  $t = 0$ , inside  $V_{\text{RX}_k}$  at time  $t$ ,  $P_{\text{ob},0}^{(\text{TX}, \text{RX}_k)}(t)$ . Given independent molecular behavior and assuming that the RXs are sufficiently far from the TX, we use [22, Eq. (6)] to write  $P_{\text{ob},0}^{(\text{TX}, \text{RX}_k)}(t)$  as

$$P_{\text{ob},0}^{(\text{TX}, \text{RX}_k)}(t) = \frac{V_{\text{RX}_k}}{(4\pi D_0 t)^{3/2}} \exp\left(-\frac{d_{\text{TX}_k}^2}{4D_0 t}\right), \quad (2)$$

where  $D_0$  is the diffusion coefficient of type  $A_0$  molecules in  $\frac{\text{m}^2}{\text{s}}$  and  $d_{\text{TX}_k}$  is the distance between the TX and  $\text{RX}_k$  in m.

We denote  $S_{\text{ob},0}^{(\text{TX}, \text{RX}_k)}[j]$  as the sum of the number of molecules observed within  $V_{\text{RX}_k}$  in the  $j$ th symbol interval, due to the emission of molecules from the current and previous symbol intervals at the TX,  $\mathbf{W}_{\text{TX}}^j$ . As discussed in [22],  $S_{\text{ob},0}^{(\text{TX}, \text{RX}_k)}[j]$  can be accurately approximated by a Poisson random variable (RV) with the mean given by

$$\begin{aligned} \bar{S}_{\text{ob},0}^{(\text{TX}, \text{RX}_k)}[j] &= S_0 \sum_{i=1}^j W_{\text{TX}}[i] \\ &\times \sum_{m=1}^{M_{\text{RX}}} P_{\text{ob},0}^{(\text{TX}, \text{RX}_k)}((j-i)T + m\Delta t_{\text{RX}}). \end{aligned} \quad (3)$$

We also denote  $U_{z,k}[j]$ ,  $z \in \{0, 1\}$ , as the conditional mean of  $S_{\text{ob},0}^{(\text{TX}, \text{RX}_k)}[j]$  when the most recent information symbol transmitted by the TX is  $W_{\text{TX}}[j] = z$ . Then, the decision at  $\text{RX}_k$  in the  $j$ th symbol interval is given by

$$\hat{W}_{\text{RX}_k}[j] = \begin{cases} 1, & \text{if } S_{\text{ob},0}^{(\text{TX}, \text{RX}_k)}[j] \geq \xi_{\text{RX}_k}, \\ 0, & \text{otherwise.} \end{cases} \quad (4)$$

<sup>3</sup>In this paper, the notations for the symbol interval time, the number of molecules for symbol “1” released by the TX, and the sampling schedules of the RXs in the perfect reporting scenario are the same as those in the noisy reporting scenario.

Moreover, based on [22, Eq. (9)], the expected MDP of the TX –  $\text{RX}_k$  link in the  $j$ th symbol interval for given  $\mathbf{W}_{\text{TX}}^{j-1}$  is written as

$$P_{\text{md},k}[j] = \Pr\left(S_{\text{ob},0}^{(\text{TX}, \text{RX}_k)}[j] < \xi_{\text{RX}_k} | W_{\text{TX}}[j] = 1, \mathbf{W}_{\text{TX}}^{j-1}\right), \quad (5)$$

and the corresponding expected FAP is written as

$$P_{\text{fa},k}[j] = \Pr\left(S_{\text{ob},0}^{(\text{TX}, \text{RX}_k)}[j] \geq \xi_{\text{RX}_k} | W_{\text{TX}}[j] = 0, \mathbf{W}_{\text{TX}}^{j-1}\right). \quad (6)$$

2) *Global Error Probability*: We consider the cooperative MC system having a symmetric topology such that the RXs have independent and *identically* distributed observations. Under this consideration, we have  $U_{z,k}[j] = U_z[j]$ . Accordingly, we assume that the decision thresholds at the RXs are the same, i.e.,  $\xi_{\text{RX}_k} = \xi_{\text{RX}}$ . Thus, we have  $P_{\text{md},k}[j] = P_{\text{md}}[j]$  and  $P_{\text{fa},k}[j] = P_{\text{fa}}[j]$ .

We first consider the  $N$ -out-of- $K$  fusion rule. Using [18, Eq. (3.4.30)] and [18, Eq. (3.4.31)] we evaluate  $Q_{\text{md}}[j]$  as

$$Q_{\text{md}}[j] = 1 - \sum_{n=N}^K \binom{K}{n} (1 - P_{\text{md}}[j])^n P_{\text{md}}[j]^{K-n} \quad (7)$$

and evaluate  $Q_{\text{fa}}[j]$  as

$$Q_{\text{fa}}[j] = \sum_{n=N}^K \binom{K}{n} P_{\text{fa}}[j]^n (1 - P_{\text{fa}}[j])^{K-n}. \quad (8)$$

For the OR rule, we obtain  $Q_{\text{md}}[j]$  and  $Q_{\text{fa}}[j]$  by substituting  $N = 1$  into (7) and (8), leading to

$$Q_{\text{md}}[j] = P_{\text{md}}[j]^K \quad (9)$$

and

$$Q_{\text{fa}}[j] = 1 - (1 - P_{\text{fa}}[j])^K, \quad (10)$$

respectively. For the AND rule, we obtain  $Q_{\text{md}}[j]$  and  $Q_{\text{fa}}[j]$  by substituting  $N = K$  into (7) and (8), resulting in

$$Q_{\text{md}}[j] = 1 - (1 - P_{\text{md}}[j])^K \quad (11)$$

and

$$Q_{\text{fa}}[j] = P_{\text{fa}}[j]^K, \quad (12)$$

respectively.

We note that the single-RX MC system, which consists of one TX, one RX, and one FC, is a special case of the cooperative MC system. Therefore, the expected error probability of the single-RX MC system in the  $j$ th symbol interval for a *given* transmitter sequence  $\mathbf{W}_{\text{TX}}^{j-1}$  in the perfect reporting scenario,  $P_{e,1}[j]$ , can be obtained by setting  $K = 1$  in (7) and (8). Accordingly, the expected average error probability of the single-RX MC system,  $\bar{P}_{e,1}$ , can be obtained by averaging  $P_{e,1}[j]$  over all possible realizations of  $\mathbf{W}_{\text{TX}}^{j-1}$  and across all symbol intervals.

#### B. Noisy Reporting

In this subsection, we first examine the error performance of the TX –  $\text{RX}_k$  – FC link, based on the analysis in [22, 25]. We then use the results of this examination to analyze  $Q_{\text{md}}[j]$  and  $Q_{\text{fa}}[j]$  in the noisy reporting scenario, enabling us to obtain  $Q_{\text{FC}}[j]$ .

1) *TX – RX<sub>k</sub> – FC Link*: We denote  $P_{\text{ob},k}^{(\text{RX}_k, \text{FC})}(t)$  as the probability of observing a given  $A_k$  molecule, emitted from the RX<sub>k</sub> at  $t = 0$ , inside  $V_{\text{FC}}$  at time  $t$ . Due to the FC's intended proximity to RX<sub>k</sub>, we find that (2) or [22, Eq. (6)] cannot be used to evaluate  $P_{\text{ob},k}^{(\text{RX}_k, \text{FC})}(t)$ . Thus, we resort to [25, Eq. (27)] to evaluate  $P_{\text{ob},k}^{(\text{RX}_k, \text{FC})}(t)$  as

$$P_{\text{ob},k}^{(\text{RX}_k, \text{FC})}(t) = \frac{1}{2} [\text{erf}(\tau_1) + \text{erf}(\tau_2)] - \frac{\sqrt{D_k t}}{d_{\text{FC},k} \sqrt{\pi}} [\exp(-\tau_1^2) - \exp(-\tau_2^2)], \quad (13)$$

where  $\tau_1 = \frac{r_{\text{FC}} + d_{\text{FC},k}}{2\sqrt{D_k t}}$ ,  $\tau_2 = \frac{r_{\text{FC}} - d_{\text{FC},k}}{2\sqrt{D_k t}}$ ,  $D_k$  is the diffusion coefficient of type  $A_k$  molecules in  $\frac{\text{m}^2}{\text{s}}$ , and  $d_{\text{FC},k}$  is the distance between RX<sub>k</sub> and the FC in m.

We denote  $S_{\text{ob},k}^{(\text{RX}_k, \text{FC})}[j]$  as the number of molecules observed within  $V_{\text{FC}}$  in the  $j$ th symbol interval, due to the emissions of molecules from the current and the previous symbol intervals at RX<sub>k</sub>,  $\mathbf{W}_{\text{RX}_k}^j$ . We note that the TX and RX<sub>k</sub> use the same modulation method and the TX – RX<sub>k</sub> and RX<sub>k</sub> – FC links are both diffusion-based. Therefore,  $S_{\text{ob},k}^{(\text{RX}_k, \text{FC})}[j]$  can be accurately approximated by a Poisson RV. We denote  $\bar{S}_{\text{ob},k}^{(\text{RX}_k, \text{FC})}[j]$  as the mean of  $S_{\text{ob},k}^{(\text{RX}_k, \text{FC})}[j]$  and obtain it by replacing  $S_0$ ,  $W_{\text{TX}}[i]$ ,  $P_{\text{ob},0}^{(\text{TX}, \text{RX}_k)}$ ,  $M_{\text{RX}_k}$ ,  $m$ , and  $\Delta t_{\text{RX}}$  with  $S_k$ ,  $\hat{W}_{\text{RX}_k}[i]$ ,  $P_{\text{ob},k}^{(\text{RX}_k, \text{FC})}$ ,  $M_{\text{FC}}$ ,  $\hat{m}$ , and  $\Delta t_{\text{FC}}$  in (3), respectively. We also denote  $V_{\bar{z},k}[j]$ ,  $\bar{z} \in \{0, 1\}$ , as the conditional mean of  $S_{\text{ob},k}^{(\text{RX}_k, \text{FC})}[j]$  when the most recent information symbol transmitted by the RX<sub>k</sub> is  $\hat{W}_{\text{RX}_k}[j] = \bar{z}$ . Furthermore, we note that  $\hat{W}_{\text{FC}}[j]$  can be obtained by replacing  $S_{\text{ob},0}^{(\text{TX}, \text{RX}_k)}[j]$  and  $\xi_{\text{RX}_k}$  with  $S_{\text{ob},k}^{(\text{RX}_k, \text{FC})}[j]$  and  $\xi_{\text{FC}}$  in (4), respectively. Thus, using [22, Eq. (13)] and [22, Eq. (14)], the expected MDP of the TX – RX<sub>k</sub> – FC link in the  $j$ th symbol interval for given  $\mathbf{W}_{\text{TX}}^{j-1}$  is derived as

$$\begin{aligned} \bar{P}_{\text{md},k}[j] = & \Pr \left( S_{\text{ob},0}^{(\text{TX}, \text{RX}_k)}[j] \geq \xi_{\text{RX}_k} | W_{\text{TX}}[j] = 1, \mathbf{W}_{\text{TX}}^{j-1} \right) \\ & \times \Pr \left( S_{\text{ob},k}^{(\text{RX}_k, \text{FC})}[j] < \xi_{\text{FC}} | \hat{W}_{\text{RX}_k}[j] = 1, \hat{\mathbf{W}}_{\text{RX}_k}^{j-1} \right) \\ & + \Pr \left( S_{\text{ob},0}^{(\text{TX}, \text{RX}_k)}[j] < \xi_{\text{RX}_k} | W_{\text{TX}}[j] = 1, \mathbf{W}_{\text{TX}}^{j-1} \right) \\ & \times \Pr \left( S_{\text{ob},k}^{(\text{RX}_k, \text{FC})}[j] < \xi_{\text{FC}} | \hat{W}_{\text{RX}_k}[j] = 0, \hat{\mathbf{W}}_{\text{RX}_k}^{j-1} \right), \quad (14) \end{aligned}$$

and the corresponding expected FAP is derived as

$$\begin{aligned} \bar{P}_{\text{fa},k}[j] = & \Pr \left( S_{\text{ob},0}^{(\text{TX}, \text{RX}_k)}[j] \geq \xi_{\text{RX}_k} | W_{\text{TX}}[j] = 0, \mathbf{W}_{\text{TX}}^{j-1} \right) \\ & \times \Pr \left( S_{\text{ob},k}^{(\text{RX}_k, \text{FC})}[j] \geq \xi_{\text{FC}} | \hat{W}_{\text{RX}_k}[j] = 1, \hat{\mathbf{W}}_{\text{RX}_k}^{j-1} \right) \\ & + \Pr \left( S_{\text{ob},0}^{(\text{TX}, \text{RX}_k)}[j] < \xi_{\text{RX}_k} | W_{\text{TX}}[j] = 0, \mathbf{W}_{\text{TX}}^{j-1} \right) \\ & \times \Pr \left( S_{\text{ob},k}^{(\text{RX}_k, \text{FC})}[j] \geq \xi_{\text{FC}} | \hat{W}_{\text{RX}_k}[j] = 0, \hat{\mathbf{W}}_{\text{RX}_k}^{j-1} \right). \quad (15) \end{aligned}$$

2) *Global Error Probability*: We consider the cooperative MC system having a symmetric topology such that the FC has independent and *identically* observations over each RX<sub>k</sub> – FC link. Under this consideration, we have  $V_{\bar{z},k}[j] = V_{\bar{z}}[j]$ . Therefore, we write  $\bar{P}_{\text{md},k}[j] = \bar{P}_{\text{md}}[j]$  and  $\bar{P}_{\text{fa},k}[j] = \bar{P}_{\text{fa}}[j]$ . In the noisy reporting scenario, we obtain  $Q_{\text{md}}[j]$  and  $Q_{\text{fa}}[j]$  for the  $N$ -out-of- $K$  rule, OR rule, and AND rule by replacing  $P_{\text{md}}[j]$  and  $P_{\text{fa}}[j]$  with  $\bar{P}_{\text{md}}[j]$  and  $\bar{P}_{\text{fa}}[j]$ , respectively, in (7)–(12). We also note that the expected error probability of the

single-RX MC system in the  $j$ th symbol interval for a *given* transmitter sequence  $\mathbf{W}_{\text{TX}}^{j-1}$  in the noisy reporting scenario can be obtained by setting  $K = 1$ .

#### IV. ERROR PERFORMANCE OPTIMIZATION

In this section, we present novel analysis to determine the joint optimal  $\xi_{\text{RX}}$  and  $\xi_{\text{FC}}$  that minimize the global error probability of the cooperative MC system. To this end, we first derive the convex upper bounds on  $Q_{\text{FC}}[j]$  for the OR rule, AND rule, and  $N$ -out-of- $K$  rule<sup>4</sup> in the perfect and noisy reporting scenarios, allowing us to formulate the corresponding convex optimization problems for given  $\mathbf{W}_{\text{TX}}^{j-1}$ . We then extend the formulated convex optimization problems for given  $\mathbf{W}_{\text{TX}}^{j-1}$  to the convex optimization problems for the *average* error performance over all possible realizations of  $\mathbf{W}_{\text{TX}}^{j-1}$  and across all symbol intervals. This extension is due to two reasons. First, optimizing the instantaneous error performance for given  $\mathbf{W}_{\text{TX}}^{j-1}$  may not be feasible in practice. This optimization mandates the precise knowledge of  $\mathbf{W}_{\text{TX}}^{j-1}$  at RX<sub>k</sub>, which cannot be realized in practice. Second, the repeated optimization of the detection threshold for each realization of  $\mathbf{W}_{\text{TX}}^{j-1}$  would demand a high computational overhead for RX<sub>k</sub>.

##### A. Perfect Reporting

In this subsection, we formulate the convex optimization problems with respect to  $\xi_{\text{RX}}$  for the OR rule, AND rule, and  $N$ -out-of- $K$  rule in the perfect reporting scenario. To achieve this, we first analyze the convexity of  $P_{\text{md}}[j]^K$  and  $P_{\text{fa}}[j]^K$  with respect to  $\xi_{\text{RX}}$ . Since  $S_{\text{ob},0}^{(\text{TX}, \text{RX}_k)}[j]$  is a Poisson RV with a discrete distribution, its convexity analysis with respect to  $\xi_{\text{RX}}$  is cumbersome. To overcome this cumbersomeness, we approximate the cumulative distribution function (CDF) of a Poisson RV  $X$  with mean  $\lambda$  by the CDF of a continuous Gaussian RV. We find that the accuracy of this approximation becomes higher when  $\lambda$  increases. Including a continuity correction, the CDF of the Gaussian RV is given by

$$\Pr(X < x) = \frac{1}{2} [1 + \Lambda(x, \lambda)], \quad (16)$$

where  $\Lambda(x, \lambda) = \text{erf}((x - 0.5 - \lambda)/\sqrt{2\lambda})$ . Applying (16) into (5) and (6),  $P_{\text{md}}[j]$  and  $P_{\text{md}}[j]$  are approximated as

$$P_{\text{md}}[j] \approx \frac{1}{2} [1 + \Lambda(\xi_{\text{RX}}, U_1[j])], \quad (17)$$

and

$$P_{\text{fa}}[j] \approx 1 - \frac{1}{2} [1 + \Lambda(\xi_{\text{RX}}, U_0[j])], \quad (18)$$

respectively. We now present the constraints making  $P_{\text{md}}[j]^K$  and  $P_{\text{fa}}[j]^K$  convex in the following theorem.

*Theorem 1*:  $P_{\text{md}}[j]^K$  and  $P_{\text{fa}}[j]^K$  are convex with respect to  $\xi_{\text{RX}}$ , if we impose the following convex constraints:

$$-0.5 - U_1[j] + \xi_{\text{RX}} \leq 0 \quad (19)$$

<sup>4</sup>We clarify that the convex upper bounds for the OR rule, AND rule, and  $N$ -out-of- $K$  rule are derived separately. This is due to the fact that the derived convex upper bounds for the  $N$ -out-of- $K$  rule with  $N = 1$  and  $N = K$  are not as tight as those derived for the OR rule and AND rule, respectively.

and

$$0.5 + U_0[j] - \xi_{\text{RX}} \leq 0, \quad (20)$$

respectively.

*Proof:* The convexity of  $P_{\text{md}}[j]^K$  can be proven by showing that its second derivative with respect to  $\xi_{\text{RX}}$  is non-negative [26]. We derive the second derivative of  $P_{\text{md}}[j]^K$  as

$$\frac{\partial^2 P_{\text{md}}[j]^K}{\partial \xi_{\text{RX}}^2} = \frac{1}{2^K} \left( \frac{2(-1+K)K}{\pi} \Xi(-2+K, 2, 1) + \sqrt{\frac{2}{\pi}} K (0.5 + U_1[j] - \xi_{\text{RX}}) \Xi\left(-1+K, 1, \frac{3}{2}\right) \right), \quad (21)$$

where

$$\Xi(\alpha, \beta, \gamma) = \frac{(1 + \Lambda(\xi_{\text{RX}}, U_1[j]))^\alpha \Theta(\xi_{\text{RX}}, U_1[j])^\beta}{U_1[j]^\gamma} \quad (22)$$

and  $\Theta(x, \lambda) \triangleq \exp\left(-\frac{(0.5 + \lambda - x)^2}{2\lambda}\right)$ . Due to the fact that the value of  $\Lambda(x, \lambda)$  is between  $-1$  and  $1$  and the value of  $\Theta(x, \lambda)$  is always greater than zero, (21) is always non-negative if we impose the constraint (19). Following a similar procedure, we prove that  $P_{\text{fa}}[j]^K$  is also convex with respect to  $\xi_{\text{RX}}$ , if we impose the constraint (20). ■

We now analyze the convexity of  $Q_{\text{fa}}[j]$  and  $Q_{\text{md}}[j]$  for the three rules. For the OR rule, an upper bound on  $Q_{\text{fa}}[j]$  is given by

$$Q_{\text{fa}}[j] \leq K P_{\text{fa}}[j], \quad (23)$$

which is obtained by applying the first degree Taylor series approximation of  $1 - (1 - P_{\text{fa}}[j])^K$  into (10) at  $P_{\text{fa}}[j] = 0$ . We find that this upper bound is tight when  $P_{\text{fa}}[j]$  is small. We note that  $P_{\text{fa}}[j]$  is convex with respect to  $\xi_{\text{RX}}$ , if we impose the constraint (20), which can be proven by considering  $K = 1$  in Theorem 1. Thus, the upper bound in (23) is also convex with respect to  $\xi_{\text{RX}}$  under the same constraint, since it scales a convex function with a non-negative constant. Also based on Theorem 1,  $Q_{\text{md}}[j]$  for the OR rule,  $P_{\text{md}}[j]^K$ , is convex with respect to  $\xi_{\text{RX}}$ , if we impose the constraint (19). Therefore, the convex optimization problem for the cooperative MC system with the OR rule in the perfect reporting scenario is formulated as

$$\begin{aligned} \min_{\xi_{\text{RX}}} \quad & P_1 P_{\text{md}}[j]^K + (1 - P_1) K P_{\text{fa}}[j] \\ \text{s.t.} \quad & (19) \text{ and } (20). \end{aligned} \quad (24)$$

Due to the convexity of the objective function and the constraints, (24) can be quickly solved by efficient algorithms, e.g., the interior-point method [26]. Throughout this paper, we refer to the optimal threshold, i.e., the threshold in the feasible set that minimizes the objective function, as the solution to the convex optimization problem, where the feasible set is the set containing all of the thresholds that satisfy all constraints.

Next, we focus on the AND rule. Using a similar method as in (23),  $Q_{\text{md}}[j]$  is upper-bounded by

$$Q_{\text{md}}[j] \leq K P_{\text{md}}[j]. \quad (25)$$

We note that  $P_{\text{md}}[j]$  is convex with respect to  $\xi_{\text{RX}}$  under the constraint (19), which can be proven by considering  $K =$

1 in Theorem 1. Thus, (25) is also convex with respect to  $\xi_{\text{RX}}$  under the same constraint. Based on Theorem 1,  $Q_{\text{fa}}[j]$  for the AND rule,  $P_{\text{fa}}[j]^K$ , is convex respect to  $\xi_{\text{RX}}$ , if we impose the constraint (20). Therefore, the convex optimization problem for the cooperative MC system with the AND rule in the perfect reporting scenario can be formulated as

$$\begin{aligned} \min_{\xi_{\text{RX}}} \quad & P_1 K P_{\text{md}}[j] + (1 - P_1) P_{\text{fa}}[j]^K \\ \text{s.t.} \quad & (19) \text{ and } (20). \end{aligned} \quad (26)$$

Finally, we consider the  $N$ -out-of- $K$  rule. We rewrite (7) as

$$Q_{\text{md}}[j] = \sum_{n=K-N+1}^K \binom{K}{n} P_{\text{md}}[j]^n (1 - P_{\text{md}}[j])^{K-n}. \quad (27)$$

Based on (27) and (8), we verify that

$$Q_{\text{md}}[j] \leq \sum_{n=K-N+1}^K \binom{K}{n} P_{\text{md}}[j]^n \triangleq Q_{\text{md}}^+[j] \quad (28)$$

and

$$Q_{\text{fa}}[j] \leq \sum_{n=N}^K \binom{K}{n} P_{\text{fa}}[j]^n \triangleq Q_{\text{fa}}^+[j]. \quad (29)$$

In Theorem 1, we showed that  $P_{\text{md}}[j]^K$  and  $P_{\text{fa}}[j]^K$  are convex with respect to  $\xi_{\text{RX}}$ , if we impose the convex constraints (19) and (20), respectively. Since (28) and (29) are non-negative weighted sums of convex functions, they are also convex with respect to  $\xi_{\text{RX}}$  under the same constraints. Therefore, the convex optimization problem for the cooperative MC system with the  $N$ -out-of- $K$  rule in the perfect reporting scenario is formulated as

$$\begin{aligned} \min_{\xi_{\text{RX}}} \quad & P_1 Q_{\text{md}}^+[j] + (1 - P_1) Q_{\text{fa}}^+[j] \\ \text{s.t.} \quad & (19) \text{ and } (20). \end{aligned} \quad (30)$$

We note that the convex optimization problem for the single-RX system in the perfect reporting scenario is a special case of problems (24), (26), and (30), with  $K = 1$ .

## B. Noisy Reporting

In this subsection, we first extend the formulated convex optimization problems from the perfect reporting scenario to the noisy reporting scenario, assuming that  $\xi_{\text{FC}}$  is fixed. We then formulate the joint convex optimization problems with respect to both  $\xi_{\text{RX}}$  and  $\xi_{\text{FC}}$  for the OR rule, AND rule, and  $N$ -out-of- $K$  rule.

1) *Optimal  $\xi_{\text{RX}}$ :* We first analyze the convexity of  $\tilde{P}_{\text{md}}[j]^K$  and  $\tilde{P}_{\text{fa}}[j]^K$  with respect to  $\xi_{\text{RX}}$ . To facilitate the convexity analysis of  $\tilde{P}_{\text{md}}[j]^K$  and  $\tilde{P}_{\text{fa}}[j]^K$  with respect to  $\xi_{\text{RX}}$ , we approximate (14) and (15) using (16), which result in

$$\begin{aligned} \tilde{P}_{\text{md}}[j] \approx \frac{1}{4} [2 + (1 + \Lambda(\xi_{\text{RX}}, U_1[j])) \Lambda(\xi_{\text{FC}}, V_0[j]) \\ + (1 - \Lambda(\xi_{\text{RX}}, U_1[j])) \Lambda(\xi_{\text{FC}}, V_1[j])] \end{aligned} \quad (31)$$

and

$$\begin{aligned} \tilde{P}_{\text{fa}}[j] \approx \frac{1}{4} [2 - (1 + \Lambda(\xi_{\text{RX}}, U_0[j])) \Lambda(\xi_{\text{FC}}, V_0[j]) \\ + (-1 + \Lambda(\xi_{\text{RX}}, U_0[j])) \Lambda(\xi_{\text{FC}}, V_1[j])], \end{aligned} \quad (32)$$

respectively. Recall that  $V_{\tilde{z},k}[j]$ ,  $\tilde{z} \in \{0,1\}$ , denotes the conditional mean of  $S_{\text{ob},k}^{(\text{RX}_k, \text{FC})}[j]$  when the most recent information symbol transmitted by the  $\text{RX}_k$  is  $\tilde{z}$ . We find that  $V_{\tilde{z}}[j]$  depends on  $\hat{\mathbf{W}}_{\text{RX}_k}^{j-1}$  and  $\hat{\mathbf{W}}_{\text{RX}_k}^{j-1}$  depends on  $\xi_{\text{RX}}$ . Thus,  $V_{\tilde{z}}[j]$  depends on  $\xi_{\text{RX}}$ , which complicates the convexity analysis of  $\tilde{P}_{\text{md}}[j]^K$  and  $\tilde{P}_{\text{fa}}[j]^K$  with respect to  $\xi_{\text{RX}}$ . To avoid this complication, we consider a constant  $V_{\tilde{z}}[j]$  in the  $j$ th symbol interval, denoted by  $\bar{V}_{\tilde{z}}[j]$ , which is averaged over all the realizations of  $\hat{\mathbf{W}}_{\text{RX}_k}^{j-1}$ , to approximate  $V_{\tilde{z}}[j]$  in (31) and (32)<sup>5</sup>. By doing so, we obtain  $\bar{V}_{\tilde{z}}[j]$  as  $\bar{V}_{\tilde{z}}[j] = \frac{1}{|\omega_j|} \sum_{\omega_j} V_{\tilde{z}}[j]$ , where  $\omega_j$  is the set containing all realizations of  $\hat{\mathbf{W}}_{\text{RX}_k}^{j-1}$  and  $|\omega_j|$  denotes the cardinality of  $\omega_j$ . Using  $\bar{V}_{\tilde{z}}[j]$ , we further approximate  $\tilde{P}_{\text{md}}[j]$  and  $\tilde{P}_{\text{fa}}[j]$  as

$$\begin{aligned} \tilde{P}_{\text{md}}[j] \approx & \frac{1}{4} [2 + (1 + \Lambda(\xi_{\text{RX}}, U_1[j])) \Lambda(\xi_{\text{FC}}, \bar{V}_0[j]) \\ & + (1 - \Lambda(\xi_{\text{RX}}, U_1[j])) \Lambda(\xi_{\text{FC}}, \bar{V}_1[j])] \end{aligned} \quad (33)$$

and

$$\begin{aligned} \tilde{P}_{\text{fa}}[j] \approx & \frac{1}{4} [2 - (1 + \Lambda(\xi_{\text{RX}}, U_0[j])) \Lambda(\xi_{\text{FC}}, \bar{V}_0[j]) \\ & + (-1 + \Lambda(\xi_{\text{RX}}, U_0[j])) \Lambda(\xi_{\text{FC}}, \bar{V}_1[j])], \end{aligned} \quad (34)$$

respectively. We now present the conditions making  $\tilde{P}_{\text{md}}[j]^K$  and  $\tilde{P}_{\text{fa}}[j]^K$  convex in the following theorem.

**Theorem 2:**  $\tilde{P}_{\text{md}}[j]^K$  and  $\tilde{P}_{\text{fa}}[j]^K$  are convex with respect to  $\xi_{\text{RX}}$  when  $\xi_{\text{FC}}$  is fixed, if we impose the convex constraints (19) and (20), respectively.

*Proof:* We derive the second derivative of  $\tilde{P}_{\text{md}}[j]^K$  as

$$\begin{aligned} \frac{\partial^2 \tilde{P}_{\text{md}}[j]^K}{\partial \xi_{\text{RX}}^2} = & (-0.5 - U_1[j] + \xi_{\text{RX}}) \Upsilon(K-1, 1, 3/2) \\ & + (K-1) \Upsilon(K-2, 2, 1) \end{aligned} \quad (35)$$

where

$$\begin{aligned} \Upsilon(\alpha, \beta, \gamma) = & \left( (1 + \Lambda(\xi_{\text{RX}}, U_1[j])) (1 + \Lambda(\xi_{\text{FC}}, \bar{V}_0[j])) \right. \\ & \left. + (1 - \Lambda(\xi_{\text{RX}}, U_1[j])) (1 + \Lambda(\xi_{\text{FC}}, \bar{V}_1[j])) \right)^\alpha \\ & \times (\Lambda(\xi_{\text{FC}}, \bar{V}_1[j]) - \Lambda(\xi_{\text{FC}}, \bar{V}_0[j]))^\beta \\ & \times \frac{K\Theta(\xi_{\text{RX}}, U_1[j])^\beta}{U_1[j]^\gamma 4^\alpha (2\sqrt{2}\pi)^\beta}. \end{aligned} \quad (36)$$

We next examine the monotonicity of  $\Lambda(\xi_{\text{FC}}, V)$  with respect to  $V$ ,  $V \in \{\bar{V}_{1,k}[j], \bar{V}_{0,k}[j]\}$ . We derive the first derivative of  $\Lambda(\xi_{\text{FC}}, \lambda)$  with respect to  $\lambda$  as

$$\frac{\partial \Lambda(\xi_{\text{FC}}, \lambda)}{\partial \lambda} = \frac{2\Theta(\xi_{\text{FC}}, \lambda)(-\xi_{\text{FC}} + 0.5 - \lambda)}{2\sqrt{2}\pi\lambda^{\frac{3}{2}}}. \quad (37)$$

Since  $\Theta(\xi_{\text{FC}}, \lambda) > 0$  and  $(-\xi_{\text{FC}} + 0.5 - \lambda) < 0$ , we find that  $\Lambda(\xi_{\text{FC}}, \lambda)$  is a monotonically decreasing function with respect to  $\lambda$ . Therefore, we have  $(\Lambda(\xi_{\text{FC}}, \bar{V}_1[j]) - \Lambda(\xi_{\text{FC}}, \bar{V}_0[j])) \leq 0$ . It follows that (35) is always non-negative if we impose

<sup>5</sup>We note that the occurrence likelihood of each realization of  $\hat{\mathbf{W}}_{\text{RX}_k}^{j-1}$  may not be the same in practice, since it depends on the value of  $\xi_{\text{RX}}$ . In this paper, we assume equal occurrence likelihood to keep a low evaluation complexity, which does not have a major impact on the analytical results.

the constraint (19), and thus  $\tilde{P}_{\text{md}}[j]^K$  is convex with respect to  $\xi_{\text{RX}}$ . Similarly, we prove that  $\tilde{P}_{\text{fa}}[j]^K$  is convex with respect to  $\xi_{\text{RX}}$ , if we impose the convex constraint (20). ■

Similar to (23) and (25), we upper-bound  $Q_{\text{fa}}[j]$  for the OR rule and  $Q_{\text{md}}[j]$  for the AND rule as

$$Q_{\text{fa}}[j] \leq K \tilde{P}_{\text{fa}}[j] \quad (38)$$

and

$$Q_{\text{md}}[j] \leq K \tilde{P}_{\text{md}}[j], \quad (39)$$

respectively. We note that  $\tilde{P}_{\text{fa}}[j]$  and  $\tilde{P}_{\text{md}}[j]$  are convex with respect to  $\xi_{\text{RX}}$ , if we impose the constraints (19) and (20), respectively, which can be proven by considering  $K = 1$  in Theorem 2. Since (38) and (39) scale a convex function with a non-negative constant, they are also convex with respect to  $\xi_{\text{RX}}$  under the same constraints. Next, we focus on  $Q_{\text{md}}[j]$  for the OR rule and  $Q_{\text{fa}}[j]$  for the AND rule. Based on Theorem 2, we note that  $\tilde{P}_{\text{md}}[j]^K$  and  $\tilde{P}_{\text{fa}}[j]^K$  are convex with respect to  $\xi_{\text{RX}}$  when  $\xi_{\text{FC}}$  is fixed, if we impose the convex constraints (19) and (20), respectively. For the  $N$ -out-of- $K$  rule, using a similar method to (27)–(29), we can derive the upper bounds on  $Q_{\text{md}}[j]$  and  $Q_{\text{fa}}[j]$  that are convex with respect to  $\xi_{\text{RX}}$ , given that  $\tilde{P}_{\text{md}}[j]^n$  and  $\tilde{P}_{\text{fa}}[j]^n$  are convex with respect to  $\xi_{\text{RX}}$ .

In the noisy reporting scenario, we formulate the convex optimization problems with respect to  $\xi_{\text{RX}}$  given fixed  $\xi_{\text{FC}}$  for the OR rule, AND rule, and  $N$ -out-of- $K$  rule by replacing  $P_{\text{md}}[j]$  and  $P_{\text{fa}}[j]$  with  $\tilde{P}_{\text{md}}[j]$  and  $\tilde{P}_{\text{fa}}[j]$ , respectively, in (24), (26), and (30). We note that the convex optimization problem with respect to  $\xi_{\text{RX}_k}$  for the single-RX system in the noisy reporting scenario is a special case of the corresponding problem for a cooperative MC system with  $K = 1$ .

**2) Joint Optimal  $\xi_{\text{RX}}$  and  $\xi_{\text{FC}}$ :** We first analyze the joint convexity of  $\tilde{P}_{\text{md}}[j]^K$  and  $\tilde{P}_{\text{fa}}[j]^K$  with respect to  $\xi_{\text{RX}}$  and  $\xi_{\text{FC}}$ . To facilitate the joint convexity analysis of  $\tilde{P}_{\text{md}}[j]^K$  and  $\tilde{P}_{\text{fa}}[j]^K$  with respect to both  $\xi_{\text{RX}}$  and  $\xi_{\text{FC}}$ , we consider the approximations given by

$$\Pr(S_{\text{ob},k}^{(\text{RX}_k, \text{FC})}[j] < \xi_{\text{FC}} | \hat{W}_{\text{RX}_k}[j] = 0, \hat{\mathbf{W}}_{\text{RX}_k}^{j-1}) \leq 1 \quad (40)$$

and

$$\Pr(S_{\text{ob},k}^{(\text{RX}_k, \text{FC})}[j] \geq \xi_{\text{FC}} | \hat{W}_{\text{RX}_k}[j] = 1, \hat{\mathbf{W}}_{\text{RX}_k}^{j-1}) \leq 1, \quad (41)$$

which are tight when the error probability of the  $\text{RX}_k - \text{FC}$  link is low. Employing (40) and (41) into (33) and (34), respectively, we further upper-bound  $\tilde{P}_{\text{md}}[j]$  and  $\tilde{P}_{\text{fa}}[j]$  as

$$\begin{aligned} \tilde{P}_{\text{mdb}}[j] = & \frac{1}{4} [3 + \Lambda(\xi_{\text{RX}}, U_1[j]) \\ & + (1 - \Lambda(\xi_{\text{RX}}, U_1[j])) \Lambda(\xi_{\text{FC}}, \bar{V}_1[j])] \end{aligned} \quad (42)$$

and

$$\begin{aligned} \tilde{P}_{\text{fab}}[j] = & \frac{1}{4} [3 - \Lambda(\xi_{\text{FC}}, \bar{V}_0[j]) \\ & - (1 + \Lambda(\xi_{\text{FC}}, \bar{V}_0[j])) \Lambda(\xi_{\text{RX}}, U_0[j])], \end{aligned} \quad (43)$$

respectively. We now present the constraints making  $\tilde{P}_{\text{mdb}}[j]^K$  and  $\tilde{P}_{\text{fab}}[j]^K$  convex in the following two theorems.



*Theorem 3:*  $\tilde{P}_{\text{mdb}}[j]^K$  is jointly convex with respect to  $\xi_{\text{RX}}$  and  $\xi_{\text{FC}}$ , if we impose the convex constraints (19), and the following constraints:

$$-0.5 - \bar{V}_1[j] + \xi_{\text{FC}} \leq 0, \quad (44)$$

$$\Phi(\xi_{\text{RX}}, \xi_{\text{FC}}^+, K) \leq 0, \text{ and } \Phi(\xi_{\text{RX}}^+, \xi_{\text{FC}}, K) \leq 0, \quad (45)$$

where  $\xi_{\text{RX}}^-$  and  $\xi_{\text{RX}}^+$  are bounds on  $\xi_{\text{RX}}$ , and  $\xi_{\text{FC}}^-$  and  $\xi_{\text{FC}}^+$  are bounds on  $\xi_{\text{FC}}$ , and  $\Phi(\mu, \nu, K)$  is given in (46) at the top of page 9.

*Theorem 4:*  $\tilde{P}_{\text{fab}}[j]^K$  is jointly convex with respect to  $\xi_{\text{RX}}$  and  $\xi_{\text{FC}}$ , if we impose the convex constraints (20) and the following constraints:

$$0.5 + \bar{V}_0[j] - \xi_{\text{FC}} \leq 0, \quad (47)$$

$$\Psi(\xi_{\text{RX}}, \xi_{\text{FC}}^-, K) \leq 0, \text{ and } \Psi(\xi_{\text{RX}}^-, \xi_{\text{FC}}, K) \leq 0, \quad (48)$$

where  $\Psi(\mu, \nu, K)$  is given in (49) at the top of page 9.

*Proof:* The proof of Theorem 3 and Theorem 4 is given in Appendix. ■

Similar to (23) and (25), we upper-bound  $Q_{\text{fa}}[j]$  for the OR rule and  $Q_{\text{md}}[j]$  for the AND rule as

$$Q_{\text{fa}}[j] \leq K \tilde{P}_{\text{fab}}[j] \quad (50)$$

and

$$Q_{\text{md}}[j] \leq K \tilde{P}_{\text{mdb}}[j], \quad (51)$$

respectively. We note that  $\tilde{P}_{\text{fab}}[j]$  is convex with respect to  $\xi_{\text{RX}}$  and  $\xi_{\text{FC}}$ , if we impose the constraints (20), (47),  $\Psi(\xi_{\text{RX}}, \xi_{\text{FC}}^-, 1) \leq 0$ , and  $\Psi(\xi_{\text{RX}}^-, \xi_{\text{FC}}, 1) \leq 0$ , which can be proven by considering  $K = 1$  in Theorem 4. We also note that  $\tilde{P}_{\text{mdb}}[j]$  is convex with respect to  $\xi_{\text{RX}}$  and  $\xi_{\text{FC}}$ , if we impose the constraints (19), (44),  $\Phi(\xi_{\text{RX}}, \xi_{\text{FC}}^+, 1) \leq 0$ , and  $\Phi(\xi_{\text{RX}}^+, \xi_{\text{FC}}, 1) \leq 0$ , which can be proven by considering  $K = 1$  in Theorem 3. Since (50) and (51) scale a convex function with a non-negative constant, they are also convex with respect to  $\xi_{\text{RX}}$  and  $\xi_{\text{FC}}$  under the same constraints. We then focus on the joint convexity analysis of  $Q_{\text{md}}[j]$  for the OR rule and  $Q_{\text{fa}}[j]$  for the AND rule. Based on Theorem 3 and Theorem 4, we note that  $\tilde{P}_{\text{mdb}}[j]^K$  and  $\tilde{P}_{\text{fab}}[j]^K$  are jointly convex with respect to  $\xi_{\text{RX}}$  and  $\xi_{\text{FC}}$ , respectively. For the  $N$ -out-of- $K$  rule, given that  $\tilde{P}_{\text{mdb}}[j]^n$  and  $\tilde{P}_{\text{fab}}[j]^n$  are jointly convex with respect to  $\xi_{\text{RX}}$  and  $\xi_{\text{FC}}$  under additional constraints, and applying a similar method to (27)–(29), we can derive the upper bounds on  $Q_{\text{md}}[j]$  and  $Q_{\text{fa}}[j]$  which are jointly convex with respect to  $\xi_{\text{RX}}$  and  $\xi_{\text{FC}}$  under the same constraints.

In the noisy reporting scenario, we formulate the convex optimization problems with respect to  $\xi_{\text{RX}}$  and  $\xi_{\text{FC}}$  for the OR rule, AND rule, and  $N$ -out-of- $K$  rule as

$$\begin{aligned} \min_{\xi_{\text{RX}}, \xi_{\text{FC}}} \quad & P_1 \tilde{P}_{\text{mdb}}[j]^K + (1 - P_1) K P_{\text{fab}}[j] \\ \text{s.t.} \quad & (19), (20), (44) - (47), \\ & \Psi(\xi_{\text{RX}}, \xi_{\text{FC}}^-, 1) \leq 0, \text{ and } \Psi(\xi_{\text{RX}}^-, \xi_{\text{FC}}, 1) \leq 0, \end{aligned} \quad (52)$$

$$\begin{aligned} \min_{\xi_{\text{RX}}, \xi_{\text{FC}}} \quad & P_1 K \tilde{P}_{\text{mdb}}[j] + (1 - P_1) \tilde{P}_{\text{fab}}[j]^K \\ \text{s.t.} \quad & (19), (20), (44), (47), (48), \\ & \Phi(\xi_{\text{RX}}^+, \xi_{\text{FC}}, 1) \leq 0, \text{ and } \Phi(\xi_{\text{RX}}, \xi_{\text{FC}}^+, 1) \leq 0, \end{aligned} \quad (53)$$

and

$$\begin{aligned} \min_{\xi_{\text{RX}}, \xi_{\text{FC}}} \quad & P_1 \tilde{Q}_{\text{md}}^+[j] + (1 - P_1) \tilde{Q}_{\text{fa}}^+[j] \\ \text{s.t.} \quad & (19), (20), (44), (47), \\ & \Phi(\xi_{\text{RX}}^+, \xi_{\text{FC}}, n) \leq 0, \Phi(\xi_{\text{RX}}, \xi_{\text{FC}}^+, n) \leq 0, \\ & \Psi(\xi_{\text{RX}}, \xi_{\text{FC}}^-, \tilde{n}) \leq 0, \text{ and } \Psi(\xi_{\text{RX}}^-, \xi_{\text{FC}}, \tilde{n}) \leq 0, \end{aligned} \quad (54)$$

respectively, where  $\tilde{Q}_{\text{md}}^+[j] \triangleq \sum_{n=K-N+1}^K \binom{K}{n} \tilde{P}_{\text{mdb}}[j]^n$  and  $\tilde{Q}_{\text{fa}}^+[j] \triangleq \sum_{\tilde{n}=N}^K \binom{K}{\tilde{n}} \tilde{P}_{\text{fab}}[j]^{\tilde{n}}$ . We note that the jointly convex optimization problem for the single-RX system in the noisy reporting scenario is a special case of problems (52), (53), and (54), with  $K = 1$ .

### C. Average Error Performance Optimization

We emphasize that the solutions to the formulated optimization problems in Sections IV-A and IV-B are the *instantaneous* suboptimal thresholds which minimize the instantaneous system error performance for given  $\mathbf{W}_{\text{TX}}^{j-1}$ . As previously explained, it may not be realistic for the RXs and FC to calculate the instantaneous suboptimal thresholds and such calculation incurs significant computational overhead. Therefore, in this subsection we aim to obtain a *single* suboptimal threshold which optimizes the average system error performance over all possible realizations of  $\mathbf{W}_{\text{TX}}^{j-1}$  and across all symbol intervals.

If we aim to optimize  $\tilde{Q}_{\text{FC}}$  for the OR rule in the perfect reporting scenario, based on (24), then we formulate the problem as

$$\begin{aligned} \min_{\xi_{\text{RX}}} \quad & \frac{1}{L} \sum_{j=1}^L \left( \frac{1}{|\omega_j|} \sum_{\omega_j} P_{\text{md}}[j]^K + K P_{\text{fa}}[j] \right) \\ \text{s.t.} \quad & \text{all constraints for all considered realizations} \\ & \text{of } \mathbf{W}_{\text{TX}}^{j-1} \text{ in } \omega_j \text{ for each symbol interval.} \end{aligned} \quad (55)$$

Using a formulation similar to (55), we can extend all convex optimization problems for optimizing the instantaneous system error performance to those for optimizing the average system error performance. Also, since all the derived inequality constraint functions are affine, the constraints define the lower limits and upper limits on  $\xi_{\text{RX}}$  and/or  $\xi_{\text{FC}}$ . We clarify that it is reasonable to only consider the minimum upper limit and the maximum lower limit on  $\xi_{\text{RX}}$  and/or  $\xi_{\text{FC}}$  among all the upper and lower limits.

## V. NUMERICAL RESULTS AND SIMULATIONS

In this section, we present numerical and simulation results to examine the error performance of the cooperative MC system. The simulation results are generated by a particle-based stochastic simulator. We also demonstrate the effectiveness of the solutions to our formulated convex optimization problems, referred to as suboptimal solutions, by comparing them with the actual optimal solutions that minimize the expected average error probability of the system. We use the fmincon solver in MATLAB with the interior-point algorithm to obtain the suboptimal solutions. We denote  $\xi_{\text{RX}}^\circ$  and  $\xi_{\text{FC}}^\circ$  as suboptimal solutions and denote  $\xi_{\text{RX}}^*$  and  $\xi_{\text{FC}}^*$  as actual optimal solutions. We refer to the minimum upper bounds achieved



$$\begin{aligned}
\Phi(\mu, \nu, K) = & 4\Theta(\xi_{\text{RX}}^+, U_1[j]) \left( -4 + K + K\Lambda(\xi_{\text{FC}}^-, \bar{V}_1[j]) + K\Lambda(\xi_{\text{RX}}^-, U_1[j]) (1 + \Lambda(\xi_{\text{FC}}^-, \bar{V}_1[j])) \right)^2 - \frac{(1 + \Lambda(\xi_{\text{RX}}^-, U_1[j]))}{\sqrt{U_1[j]\bar{V}_1[j]}} \\
& \times (1 + \Lambda(\xi_{\text{FC}}^-, \bar{V}_1[j])) \left( 2(-1 + K) \sqrt{\bar{V}_1[j]} (1 + \Lambda(\xi_{\text{RX}}^+, U_1[j])) - \frac{\sqrt{2\pi}}{\Theta(\xi_{\text{FC}}^+, \bar{V}_1[j])} (0.5 + \bar{V}_1[j] - \nu) \right. \\
& \times (-3 + \Lambda(\xi_{\text{FC}}^+, \bar{V}_1[j]) + \Lambda(\xi_{\text{RX}}^+, U_1[j]) (1 + \Lambda(\xi_{\text{FC}}^+, \bar{V}_1[j]))) \left( \Theta(\xi_{\text{RX}}^+, U_1[j]) (1 + \Lambda(\xi_{\text{FC}}^-, \bar{V}_1[j])) \right. \\
& \times (-1 + K) 2\sqrt{U_1[j]} - \sqrt{2\pi} (0.5 + U_1[j] - \mu) (-3 + \Lambda(\xi_{\text{FC}}^+, \bar{V}_1[j]) + \Lambda(\xi_{\text{RX}}^+, U_1[j]) (1 + \Lambda(\xi_{\text{FC}}^+, \bar{V}_1[j]))) \left. \right) \quad (46)
\end{aligned}$$

$$\begin{aligned}
\Psi(\mu, \nu, K) = & 4\Theta(\xi_{\text{RX}}^-, U_0[j]) \left( -4 + K - K\Lambda(\xi_{\text{FC}}^+, \bar{V}_0[j]) + K\Lambda(\xi_{\text{RX}}^+, U_0[j]) (-1 + \Lambda(\xi_{\text{FC}}^+, \bar{V}_0[j])) \right)^2 - \frac{(1 - \Lambda(\xi_{\text{RX}}^+, U_0[j]))}{\sqrt{U_0[j]\bar{V}_0[j]}} \\
& \times (-1 + \Lambda(\xi_{\text{FC}}^-, \bar{V}_0[j])) \left( -2(-1 + K) \sqrt{\bar{V}_0[j]} (-1 + \Lambda(\xi_{\text{RX}}^-, U_0[j])) + \frac{\sqrt{2\pi}}{\Theta(\xi_{\text{FC}}^-, \bar{V}_0[j])} (0.5 + \bar{V}_0[j] - \nu) \right. \\
& \times (-3 - \Lambda(\xi_{\text{FC}}^+, \bar{V}_0[j]) + \Lambda(\xi_{\text{RX}}^-, U_0[j]) (-1 + \Lambda(\xi_{\text{FC}}^-, \bar{V}_0[j]))) \left( \Theta(\xi_{\text{RX}}^-, U_0[j]) (-1 + \Lambda(\xi_{\text{FC}}^-, \bar{V}_0[j])) \right. \\
& \times (-1 + K) 2\sqrt{U_0[j]} - \sqrt{2\pi} (0.5 + U_0[j] - \mu) (-3 - \Lambda(\xi_{\text{FC}}^-, \bar{V}_0[j]) + \Lambda(\xi_{\text{RX}}^-, U_0[j]) (-1 + \Lambda(\xi_{\text{FC}}^+, \bar{V}_0[j]))) \left. \right) \quad (49)
\end{aligned}$$

TABLE I  
FIXED ENVIRONMENTAL PARAMETERS USED IN SECTION V

Parameter	Symbol	Value
Radius of RXs	$r_{\text{RX}_k}$	$0.225 \mu\text{m}$
Radius of FC	$r_{\text{FC}}$	$0.200 \mu\text{m}$
Time step at RXs	$\Delta t_{\text{RX}}$	$100 \mu\text{s}$
Time step at FC	$\Delta t_{\text{FC}}$	$30 \mu\text{s}$
Number of samples of RXs	$M_{\text{RX}}$	5
Number of samples of FC	$M_{\text{FC}}$	5
Transmission time interval	$t_{\text{trans}}$	1 ms
Report time interval	$t_{\text{report}}$	0.3 ms
Bit interval time	$T$	1.3 ms
Diffusion coefficient	$D_0 = D_k$	$5 \times 10^{-9} \text{m}^2/\text{s}$
Length of symbol sequence	$L$	10
Probability of binary 1	$P_1$	0.5

by  $\xi_{\text{RX}}^\circ$  and  $\xi_{\text{FC}}^\circ$  as suboptimal error probabilities. We refer to the expected error probability achieved by  $\xi_{\text{RX}}^\circ$  and  $\xi_{\text{FC}}^\circ$  as the approximated error probabilities.

We list all the fixed environmental parameters adopted in this section in Table I. The varying parameters adopted in this section are the decision threshold at RXs,  $\xi_{\text{RX}}$ , the decision threshold at the FC,  $\xi_{\text{FC}}$ , the number of RXs,  $K$ , and the radius of the FC,  $r_{\text{FC}}$ . In particular,  $r_{\text{FC}}$  is fixed at  $0.200 \mu\text{m}$  in all the figures except for Fig. 6. In the following, we assume that the TX releases  $S_0 = 8000$  molecules for information symbol “1” and the total number of molecules released by all RXs for symbol “1” is fixed at 2000, i.e., each RX releases  $S_k = 2000/K$  molecules to report its decision of symbol “1”. The locations of the TX, RXs, and FC are listed in Table II. For each realization of  $\mathbf{W}_{\text{TX}}^{j-1}$ , we set  $\xi_{\text{RX}}^- = U_0[j] + 1$ ,  $\xi_{\text{RX}}^+ = U_1[j]$ ,  $\xi_{\text{FC}}^- = \bar{V}_0[j] + 1$ , and  $\xi_{\text{FC}}^+ = \bar{V}_1[j]$ , since the initial convex feasible sets of  $\xi_{\text{RX}}$  and  $\xi_{\text{FC}}$  are  $0.5 + U_0[j] \leq \xi_{\text{RX}} \leq 0.5 + U_1[j]$  and  $0.5 + \bar{V}_0[j] \leq \xi_{\text{FC}} \leq 0.5 + \bar{V}_1[j]$ , respectively.

Throughout this section,  $\bar{Q}_{\text{FC}}$  are calculated by averaging  $P_{e,k}[j]$  and  $Q_{\text{FC}}[j]$ , respectively, over all considered realizations

TABLE II  
LOCATIONS OF TX, RXS, AND FC

Devices	X-axis [ $\mu\text{m}$ ]	Y-axis [ $\mu\text{m}$ ]	Z-axis [ $\mu\text{m}$ ]
TX	0	0	0
RX <sub>1</sub>	2	0.6	0
RX <sub>2</sub>	2	-0.6	0
RX <sub>3</sub>	2	0	0.6
RX <sub>4</sub>	2	0	-0.6
RX <sub>5</sub>	2	0.3	0.5196
RX <sub>6</sub>	2	0.3	-0.5196
FC	2	0	0

of  $\mathbf{W}_{\text{TX}}^{j-1}$  and across all symbol intervals. Here, we consider all possible realizations of  $\mathbf{W}_{\text{TX}}^{j-1}$  except for the realization of all “0” bits, i.e., when the MDP is zero and there is no optimal threshold. Since we consider the length of the symbol sequence from the TX is 10 bits, we consider 1023 different symbol sequences in total. The simulated error probabilities are averaged over at least  $5 \times 10^4$  independent transmissions of the considered symbol sequences. In Figs. 2–4, we plot the simulation for the expected error probabilities, while in Fig. 6, we plot the simulation for the approximated error probabilities. Moreover, we clarify that  $\xi_{\text{RX}}^\circ$  and  $\xi_{\text{FC}}^\circ$  for the expected average error probabilities are obtained by performing the optimization method in Section IV-C only *once*, unless otherwise noted. Furthermore, we clarify that the non-integer optimization solutions are rounded to integers in Figs. 3, 5, and 6. Specifically, the most two nearest integers around the solution are compared and the one achieving the lower error probability is chosen.

#### A. Perfect Reporting

In this subsection we consider the *perfect* reporting scenario. In Fig. 2, we consider a three-RX cooperative system and plot the average global error probability versus the decision threshold at the RXs for the OR rule, AND rule, and majority

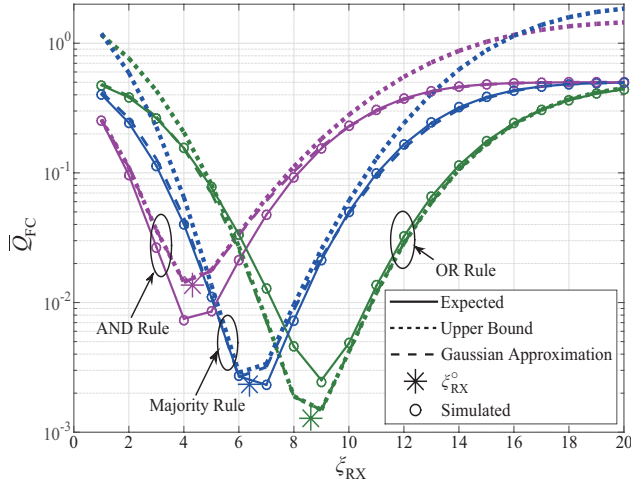


Fig. 2. Average global error probability  $\overline{Q}_{FC}$  of different fusion rules versus the decision threshold at RXs  $\xi_{RX}$  with  $K=3$  in the perfect reporting scenario.

rule. The expected curves for the three rules are obtained from (7)–(12) with (5) and (6). The Gaussian approximation curves for the three rules are obtained from (7)–(12) with (17) and (18). The upper bound curves for the OR rule, AND rule, and majority rule are obtained from (9) and (23), (12) and (25), and (28) and (29), respectively, with (17) and (18). The value of  $\xi_{RX}^o$  for the OR rule, AND rule, and majority rule is obtained by solving (24), (26), and (30), respectively, with (17) and (18).

In Fig. 2, we first observe that the simulated points accurately match the expected curves, validating our analysis of the expected results. Second, we observe that  $\xi_{RX}^o$  is almost identical to  $\xi_{RX}^*$  for each fusion rule, confirming the accuracy of  $\xi_{RX}^o$ . Third, we observe that the Gaussian approximation curves well approximate the expected curves. Fourth, we observe that the convex upper bound curve for the OR rule is lower than its expected curve. This can be explained as follows: In the single-RX system, the Gaussian approximations give an upper bound on  $P_{md}[j]$  and a lower bound on  $P_{fa}[j]$ . For the OR rule,  $Q_{md}[j]$  is the product of  $P_{md}[j]$  and  $Q_{fa}[j]$  is the sum of  $P_{fa}[j]$ . Since the Gaussian approximation of  $Q_{md}[j]$  is tighter than that of  $Q_{fa}[j]$ , the Gaussian approximation of the global error probability for the OR rule is lower than the expected curve. Finally, observing the expected curves, we find that the majority rule outperforms the OR rule and the OR rule outperforms the AND rule at their corresponding optimal decision thresholds.

In Fig. 3, we plot the optimal average global error probability versus the number of cooperative RXs for the OR, AND, and majority rules. The baseline case is a single TX – RX link with  $K=1$ , i.e., only one RX exists but no FC exists. In the baseline case, we assume that the RX is located at  $(2\mu m, 0.6\mu m, 0)$ , the TX releases 10000 molecules, the time step between two successive samples is  $100\mu s$ , and the symbol interval time is  $T=1.3ms$ , all of which ensure the fairness of the error performance comparison between the baseline case and the considered cooperative MC system. The value of  $\overline{Q}_{FC}^*$  for each  $K$  in the expected curves for the three fusion rules is

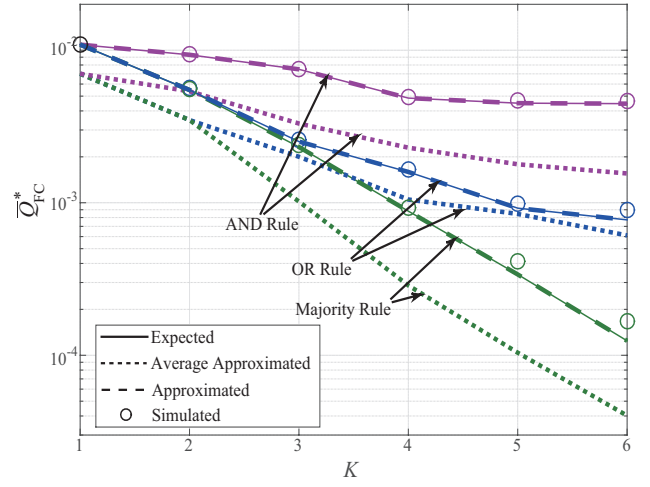


Fig. 3. Optimal average global error probability  $\overline{Q}_{FC}^*$  of different fusion rules versus the number of cooperative RXs  $K$  in the perfect reporting scenario.

the minimum  $\overline{Q}_{FC}$ . For the expected curves, we consider that a single  $\xi_{RX}^*$  is applied to all considered realizations of  $\mathbf{W}_{TX}^{j-1}$ , which are obtained via exhaustive search of the expected expressions of (7)–(12) with (5) and (6). On the other hand, the value of  $\overline{Q}_{FC}^*$  for each  $K$  in the approximated curves for the OR rule, AND rule, and majority rule are obtained by solving the corresponding average error performance optimization problems given by (24), (26), and (30), respectively. To this end, we use a single  $\xi_{RX}^o$  for all considered realizations of  $\mathbf{W}_{TX}^{j-1}$ , and then calculate the actual values of  $\overline{Q}_{FC}$  achieved by  $\xi_{RX}^o$ . The value of  $\overline{Q}_{FC}$  for each  $K$  in the average approximated curves are obtained by solving (24), (26), and (30), respectively, with (17) and (18) for all considered realizations. For this purpose, we consider a single  $\xi_{RX}^o$  for each realization of  $\mathbf{W}_{TX}^{j-1}$ . We then calculate the actual value of  $Q_{FC}[j]$  achieved by  $\xi_{RX}^o$  for each realization of  $\mathbf{W}_{TX}^{j-1}$ , and refer to it as the instantaneous approximated error probabilities. Finally, we calculate the mean of all the instantaneous approximated error probabilities for all realizations of  $\mathbf{W}_{TX}^{j-1}$ .

In Fig. 3, we first observe that for the OR rule, AND rule, and majority rule, the approximated curves match the expected curves, which confirms the accuracy of  $\xi_{RX}^o$ . Second, we observe an accurate match between the simulated points and the expected curves, except for  $K=6$  for the majority rule. The gap between the simulated point and the expected curve for the majority rule with  $K=6$  is caused by the insufficient number of simulations. Third, we observe that for the three fusion rules, the error performance clearly improves when the optimization is performed for each realization of  $\mathbf{W}_{TX}^{j-1}$ . However, as previously explained, this performance gain may not be feasible in practice and thus, we consider the average approximated curves as the best performance bound of our considered system. Fourth, we observe from the expected curves that the majority rule outperforms the OR rule and AND rule, which is consistent with that in Fig. 2. Lastly, we observe that the cooperative MC system outperforms the baseline case for all fusion rules, even though the distance of the baseline case is shorter than that of the cooperative MC

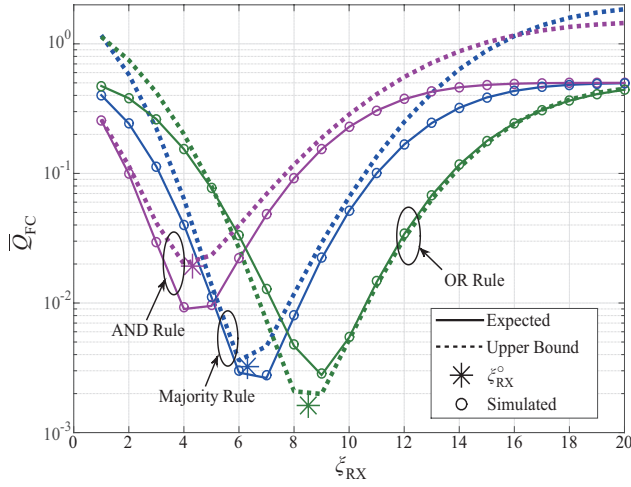


Fig. 4. Average global error probability  $\bar{Q}_{FC}$  of different fusion rules versus the decision threshold at RXs  $\xi_{RX}$  with  $K = 3$  in the noisy reporting scenario.

system. Importantly, we see that the system error performance significantly improves as  $K$  increases. This is due to fact that an increasing number of cooperative RXs enables more independent observations of the transmitted information symbol. It follows that the probability that all RXs fail to detect the transmitted information symbol is reduced.

### B. Noisy Reporting

In this subsection we focus on the *noisy* reporting scenario. In Fig. 4, we consider a three-RX cooperative system and plot the average global error probability versus the decision threshold at the RXs for the AND rule, OR rule, and majority rule. In this figure, we consider the fixed optimal threshold at the FC for the three fusion rules, given by  $\xi_{FC} = 2$  for the AND rule,  $\xi_{FC} = 4$  for the OR rule, and  $\xi_{FC} = 3$  for the majority rule. All curves in this figure are obtained from the same expressions and the same optimization problems as those in Fig. 2, except for replacing (5), (6), (17), and (18) with (14), (15), (33), and (34), respectively. Similar to Fig. 2, we observe that  $\xi_{RX}^o$  is almost identical to  $\xi_{RX}^*$ . We also observe that the expected error probabilities in Fig. 4 are slightly higher than those in Fig. 2. This observation is not surprising since we account for the error probability of the  $RX_k - FC$  link and the relatively short distance between the  $RX_k$  and the FC leads to a relatively low error probability in the  $RX_k - FC$  link. This low error probability does not significantly affect the error probability of the  $TX - RX_k - FC$  link. In addition, we also confirmed that increasing  $K$  significantly improves the system error performance in the noisy reporting scenario (figure omitted for brevity).

In Fig. 5, we consider a three-RX cooperative system and plot the expected average global error probability versus the decision thresholds at the RXs and FC for the OR rule, AND rule, and majority rule in Fig. 5(a), Fig. 5(b), and Fig. 5(c), respectively. The expected surfaces for the three fusion rules are obtained from (7)–(12) with (14) and (15). The values of  $\xi_{RX}^o$  and  $\xi_{FC}^o$ , associated with ‘■’, for the OR rule, AND rule, and majority rule are obtained by solving (52), (53), and (54),

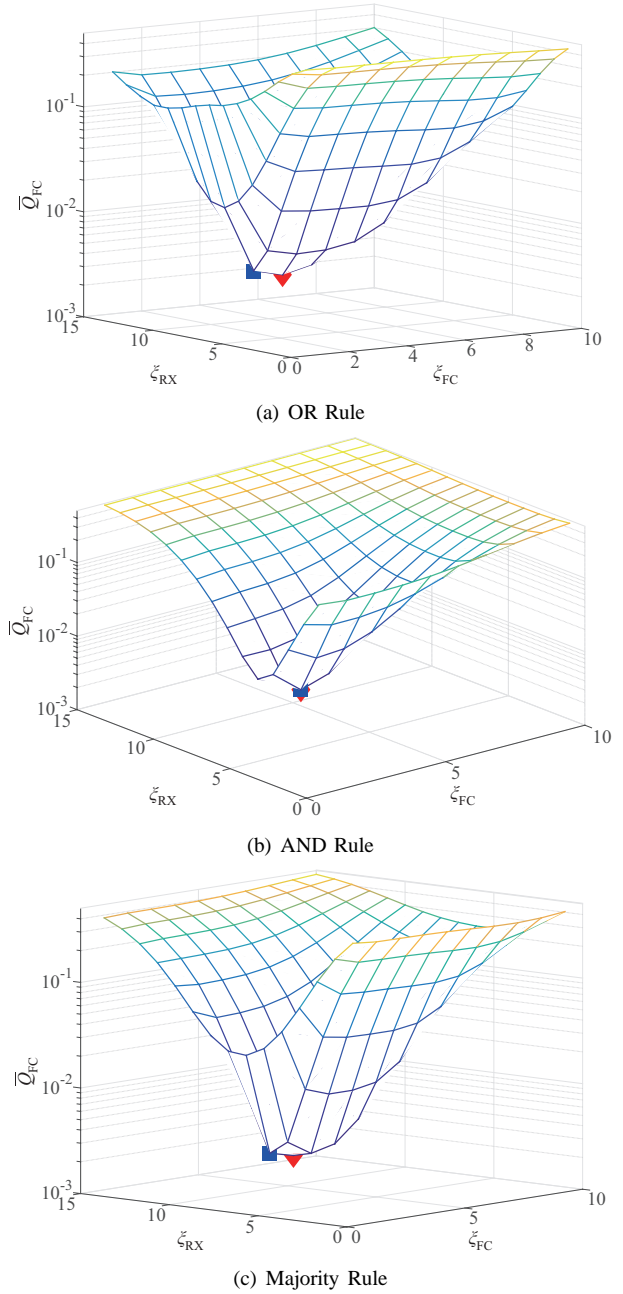


Fig. 5. Expected average global error probability  $\bar{Q}_{FC}$  versus the decision threshold at RXs  $\xi_{RX}$  and the decision threshold at the FC  $\xi_{FC}$  with  $K = 3$  in the noisy reporting scenario for (a) OR rule, (b) AND rule, and (c) majority rule. In (a)–(c), ‘♦’ is the optimal  $\bar{Q}_{FC}$  achieved by  $\xi_{RX}^*$  and  $\xi_{FC}^*$ , obtained by exhaustive search, and ‘■’ is the approximated  $\bar{Q}_{FC}$  achieved by  $\xi_{RX}^o$  and  $\xi_{FC}^o$ .

TABLE III  
COORDINATES AND VALUES OF ‘♦’ AND ‘■’ IN FIG. 5

Variable	OR Rule	AND rule	Majority Rule
$\xi_{FC}^*$ of ‘♦’	4	2	3
$\xi_{RX}^*$ of ‘♦’	9	4	7
$\xi_{FC}^o$ of ‘■’	3	2	2
$\xi_{RX}^o$ of ‘■’	9	4	7
Value of ‘♦’	$2.78 \times 10^{-3}$	$8.99 \times 10^{-3}$	$2.64 \times 10^{-3}$
Value of ‘■’	$3.22 \times 10^{-3}$	$8.99 \times 10^{-3}$	$3.01 \times 10^{-3}$

respectively. The coordinates and values of ‘♦’ and ‘■’ in Figs. 5(a), 5(b), and 5(c) are summarized in Table III. Based

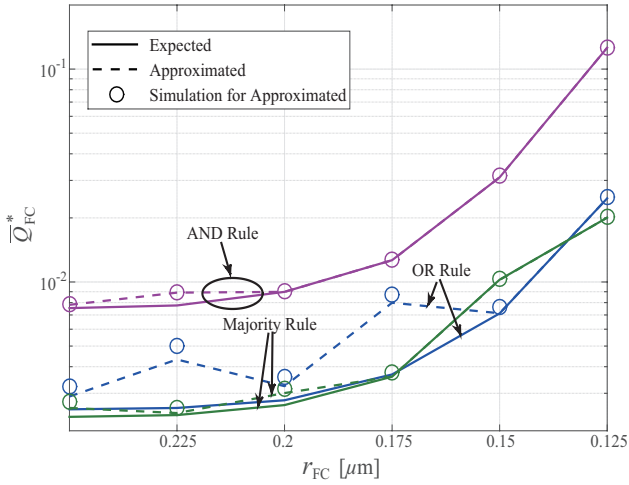


Fig. 6. Optimal average global error probability  $\bar{Q}_{FC}^*$  of different fusion rules versus the radius of the FC  $r_{FC}$  with  $K = 3$  in the noisy reporting scenario.

on Table III, we quantify the accuracy loss caused by the suboptimal convex optimization for the OR rule, AND rule, and majority rule as 15.7%, 0%, and 14%, respectively. These small losses reveal that the joint  $\xi_{RX}^o$  and  $\xi_{FC}^o$  we find can achieve near-optimal error performance.

In Fig. 6, we consider a three-RX cooperative system and plot the average global error probability versus the radius of the FC for the AND rule, OR rule, and majority rule. The value of  $\bar{Q}_{FC}^*$  for each  $r_{FC}$  in the expected curves for the three fusion rules are obtained via the exhaustive search of (7)–(12) with (14) and (15). The value of  $\bar{Q}_{FC}^*$  for each  $r_{FC}$  in the approximated curves for the three fusion rules are obtained by first solving (52), (53), and (54), respectively, and then searching the actual values of  $\bar{Q}_{FC}$  achieved by  $\xi_{RX}^o$  and  $\xi_{FC}^o$ . The simulation for approximated curves are obtained by considering  $\xi_{RX}^o$  and  $\xi_{FC}^o$  for each  $r_{FC}$ . We observe that for the AND rule and majority rule, the approximated curves well approximate the expected curves, which confirms the accuracy of jointly optimizing  $\xi_{RX}^o$  and  $\xi_{FC}^o$ . We also observe that for the OR rule, the approximated curve deviates from the expected curve when  $r_{FC} = 0.225$  and  $r_{FC} = 0.175$ . This is due to the fact that the global error probability is very sensitive to both thresholds in the region of  $\xi_{FC}^*$ . Furthermore, we observe that the approximated curves match the expected curves when  $r_{FC} \leq 0.2\mu\text{m}$  for the AND rule,  $r_{FC} \leq 0.15\mu\text{m}$  for the OR rule, and  $r_{FC} \leq 0.175\mu\text{m}$  for the majority rule. Additionally, we observe that the expected error performance degrades as  $r_{FC}$  decreases for all the fusion rules. This can be explained by the fact that the reporting from the RXs to the FC becomes less reliable when  $r_{FC}$  decreases.

## VI. CONCLUSIONS

In this paper, we optimized the error performance achieved by cooperative detection among distributed receivers in a diffusion-based MC system. For the perfect and noisy reporting scenarios, we derived closed-form expressions for the expected global error probability of the system having a symmetric topology. We also derived approximated expressions

for the expected error probability in both reporting scenarios. We then found the convex constraints under which the approximated expressions are jointly convex with respect to the decision thresholds at the receivers and the FC. Based on the derived convex approximations and constraints, we formulated suboptimal convex optimization problems for the system in both reporting scenarios. Furthermore, we extended the suboptimal convex optimization problem for the instantaneous error performance to that for the average error performance over all transmitter symbol sequences. Using numerical and simulation results, we showed that the system error performance can be significantly improved by combining the detection information among distributed receivers, even when the total number of transmitted molecules is limited. We also showed that the suboptimal decision thresholds, obtained by solving our formulated convex optimization problems, achieve near-optimal global error performance. In our future work, we will explore the error performance analysis and optimization of soft fusion schemes at the fusion centre and the cooperative MC system with an asymmetric topology.

## APPENDIX

### PROOF OF THEOREM 3 AND THEOREM 4

The convexity of  $\tilde{P}_{mdb}[j]^K$  can be proven by showing that its Hessian is positive semidefinite (PSD) [26]. Although the Hessian of  $\tilde{P}_{mdb}[j]^K$  is not always PSD, we can show that the Hessian of  $\tilde{P}_{mdb}[j]^K$  is PSD over a convex region if we impose a set of additional constraints. Recall that a matrix is PSD if and only if all of its principal minors are non-negative [27]. Thus, we prove the joint convexity of  $\tilde{P}_{mdb}[j]^K$  with respect to  $\xi_{RX}$  and  $\xi_{FC}$  by finding when  $\frac{\partial^2 \tilde{P}_{mdb}[j]^K}{\partial \xi_{RX}^2} \geq 0$ ,  $\frac{\partial^2 \tilde{P}_{mdb}[j]^K}{\partial \xi_{FC}^2} \geq 0$ , and  $\left(\frac{\partial^2 \tilde{P}_{mdb}[j]^K}{\partial \xi_{RX}^2}\right) \left(\frac{\partial^2 \tilde{P}_{mdb}[j]^K}{\partial \xi_{FC}^2}\right) - \left(\frac{\partial^2 \tilde{P}_{mdb}[j]^K}{\partial \xi_{RX} \partial \xi_{FC}}\right)^2 \geq 0$ .

We derive the second partial derivatives of  $\tilde{P}_{mdb}[j]^K$  with respect to  $\xi_{RX}$  and  $\xi_{FC}$  as

$$\begin{aligned} \frac{\partial^2 \tilde{P}_{mdb}[j]^K}{\partial \xi_{RX}^2} &= \Gamma(\xi_{RX}, \xi_{FC}, U_1[j], \bar{V}_1[j]) \\ &= (-0.5 - U_1[j] + \xi_{RX}) \hat{\Upsilon}(K-1, 1, 3/2) \\ &\quad + (K-1) \hat{\Upsilon}(K-2, 2, 1) \end{aligned} \quad (56)$$

and

$$\frac{\partial^2 \tilde{P}_{mdb}[j]^K}{\partial \xi_{FC}^2} = \Gamma(\xi_{FC}, \xi_{RX}, \bar{V}_1[j], U_1[j]), \quad (57)$$

respectively, where

$$\begin{aligned} \hat{\Upsilon}(\alpha, \beta, \gamma) &= \left( (1 - \Lambda(\xi_{RX}, U_1[j])) (1 + \Lambda(\xi_{FC}, \bar{V}_1[j])) \right. \\ &\quad \left. + 2(1 + \Lambda(\xi_{RX}, U_1[j])) \right)^\alpha (\Lambda(\xi_{FC}, \bar{V}_1[j]) - 1)^\beta \\ &\quad \times \frac{K \Theta(\xi_{RX}, U_1[j])^\beta}{U_1[j] \gamma 4^\alpha (2\sqrt{2}\pi)^\beta}. \end{aligned} \quad (58)$$

Since  $\Lambda(x, \lambda)$  is between  $-1$  and  $1$  and  $\Theta(x, \lambda)$  is greater than zero, (56) and (57) are always non-negative if we impose the convex constraints (19) and (44), respectively.

$$\begin{aligned}
\Omega(\xi_{\text{RX}}, \xi_{\text{FC}}) = & -4\Theta(\xi_{\text{RX}}, U_1[j])(-4 + K + K\Lambda(\xi_{\text{FC}}, \bar{V}_1[j]) + K\Lambda(\xi_{\text{RX}}, U_1[j])(1 + \Lambda(\xi_{\text{FC}}, \bar{V}_1[j])))^2 + \frac{(1 + \Lambda(\xi_{\text{RX}}, U_1[j]))}{\sqrt{U_1[j]\bar{V}_1[j]}} \\
& \times (1 + \Lambda(\xi_{\text{FC}}, \bar{V}_1[j])) \left( 2(-1 + K)\sqrt{\bar{V}_1[j]}(1 + \Lambda(\xi_{\text{RX}}, U_1[j])) - \frac{\sqrt{2\pi}}{\Theta(\xi_{\text{FC}}, \bar{V}_1[j])}(0.5 + \bar{V}_1[j] - \xi_{\text{FC}}) \right. \\
& \times (-3 + \Lambda(\xi_{\text{FC}}, \bar{V}_1[j]) + \Lambda(\xi_{\text{RX}}, U_1[j])(1 + \Lambda(\xi_{\text{FC}}, \bar{V}_1[j]))) \left( \Theta(\xi_{\text{RX}}, U_1[j])(-1 + K)(1 + \Lambda(\xi_{\text{FC}}, \bar{V}_1[j])) \right. \\
& \times 2\sqrt{U_1[j]} - \sqrt{2\pi}(0.5 + U_1[j] - \xi_{\text{RX}})(-3 + \Lambda(\xi_{\text{FC}}, \bar{V}_1[j]) + \Lambda(\xi_{\text{RX}}, U_1[j])(1 + \Lambda(\xi_{\text{FC}}, \bar{V}_1[j]))) \left. \right) \quad (59)
\end{aligned}$$

Finally, we show how the third condition of the joint convexity is satisfied. To this end, we derive the second mixed derivative of  $\tilde{P}_{\text{mdb}}[j]^K$  with respect to  $\xi_{\text{RX}}$  and  $\xi_{\text{FC}}$  as

$$\begin{aligned}
\frac{\partial^2 \tilde{P}_{\text{mdb}}[j]^K}{\partial \xi_{\text{RX}} \partial \xi_{\text{FC}}} = & \frac{2^{1-2K} K}{\pi \sqrt{U_1[j]\bar{V}_1[j]}} \Theta(\xi_{\text{RX}}, U_1[j]) \Theta(\xi_{\text{FC}}, \bar{V}_1[j]) \\
& \times \left( 3 - \Lambda(\xi_{\text{RX}}, U_1[j])(1 + \Lambda(\xi_{\text{FC}}, \bar{V}_1[j])) \right. \\
& \left. - \Lambda(\xi_{\text{FC}}, \bar{V}_1[j]) \right)^{-2+K} \left( -4 + K \right. \\
& \left. + K\Lambda(\xi_{\text{FC}}, \bar{V}_1[j]) + K\Lambda(\xi_{\text{RX}}, U_1[j]) \right. \\
& \left. \times (1 + \Lambda(\xi_{\text{FC}}, \bar{V}_1[j])) \right). \quad (60)
\end{aligned}$$

Combining (56), (57), and (60), and performing some algebraic manipulations, we have

$$\begin{aligned}
& \left( \frac{\partial^2 \tilde{P}_{\text{mdb}}[j]^K}{\partial \xi_{\text{RX}}^2} \right) \left( \frac{\partial^2 \tilde{P}_{\text{mdb}}[j]^K}{\partial \xi_{\text{FC}}^2} \right) - \left( \frac{\partial^2 \tilde{P}_{\text{mdb}}[j]^K}{\partial \xi_{\text{RX}} \partial \xi_{\text{FC}}} \right)^2 \\
= & \Omega(\xi_{\text{RX}}, \xi_{\text{FC}}) \frac{K^2 2^{-4K}}{\pi^2 U_1[j]\bar{V}_1[j]} \Theta(\xi_{\text{FC}}, \bar{V}_1[j]) \Theta(\xi_{\text{RX}}, U_1[j]) \\
& \times \left( 3 - \Lambda(\xi_{\text{FC}}, \bar{V}_1[j]) - \Lambda(\xi_{\text{RX}}, U_1[j]) \right. \\
& \left. \times (1 + \Lambda(\xi_{\text{FC}}, \bar{V}_1[j])) \right)^{(-4+2K)}, \quad (61)
\end{aligned}$$

where  $\Omega(\xi_{\text{RX}}, \xi_{\text{FC}})$  is shown at the top of page 13.

We note that (61) is always non-negative if the following constraint is satisfied:

$$\Omega(\xi_{\text{RX}}, \xi_{\text{FC}}) \geq 0. \quad (62)$$

The constraint (62) is not convex, and  $\xi_{\text{RX}}$  and  $\xi_{\text{FC}}$  in the exponential and error functions make joint convexity analysis with respect to  $\xi_{\text{RX}}$  and  $\xi_{\text{FC}}$  cumbersome. To tackle this cumbersomeness, we can bound  $\xi_{\text{RX}}$  with  $\xi_{\text{RX}}^-$  or  $\xi_{\text{RX}}^+$ , and bound  $\xi_{\text{FC}}$  with  $\xi_{\text{FC}}^-$  or  $\xi_{\text{FC}}^+$  to lower the value of the left-hand side of (62). Thus, we obtain (45) to ensure that (61) is always non-negative. Under the constraints (19), (44), and (45), we define a convex region where  $\tilde{P}_{\text{mdb}}[j]^K$  is jointly convex with respect to  $\xi_{\text{FC}}$  and  $\xi_{\text{RX}}$ .

Similar to the proof of the joint convexity of  $\tilde{P}_{\text{mdb}}[j]^K$ , it can be proven that  $\tilde{P}_{\text{fab}}[j]^K$  is also jointly convex with respect to  $\xi_{\text{RX}}$  and  $\xi_{\text{FC}}$  under the constraints (20), (47), and (48).

## REFERENCES

- [1] Y. Fang, A. Noel, N. Yang, A. W. Eckford, and R. A. Kennedy, "Distributed cooperative detection for multi-receiver molecular communication," in *Proc. IEEE GLOBECOM 2016*, Washington, DC, Dec. 2016.
- [2] I. F. Akyildiz, F. Brunetti, and C. Blazquez, "Nanonetworks: A new communication paradigm," *Comput. Networks*, vol. 52, no. 12, pp. 2260–2279, May 2008.
- [3] T. Nakano, M. J. Moore, F. Wei, A. V. Vasilakos, and J. Shuai, "Molecular communication and networking: Opportunities and challenges," *IEEE Trans. NanoBiosci.*, vol. 11, no. 2, pp. 135–148, June 2012.
- [4] T. Nakano, A. W. Eckford, and T. Haraguchi, *Molecular Communication*. Cambridge, UK: Cambridge University Press, 2013.
- [5] N. Farsad, H. B. Yilmaz, A. Eckford, C.-B. Chae, and W. Guo, "A comprehensive survey of recent advancements in molecular communication," *IEEE Commun. Surveys & Tutorials*, vol. 18, no. 3, pp. 1887–1919, Aug. 2016.
- [6] B. Atakan and O. B. Akan, "Single and multiple-access channel capacity in molecular nanonetworks," in *Proc. ICST Nano-Net 2009*, Luzern, Switzerland, Mar. 2009, pp. 14–23.
- [7] M. T. Barros, S. Balasubramaniam, and B. Jennings, "Comparative end-to-end analysis of  $\text{Ca}^{2+}$ -signaling-based molecular communication in biological tissues," *IEEE Trans. Commun.*, vol. 63, no. 12, pp. 5128–5142, Dec. 2015.
- [8] S. M. Baylor and S. Hollingworth, "Calcium indicators and calcium signalling in skeletal muscle fibres during excitation-contraction coupling," *Prog. Biophys. Mol. Biol.*, vol. 105, pp. 162–179, June 2010.
- [9] B. Atakan and O. B. Akan, "On molecular multiple-access, broadcast, and relay channels in nanonetworks," in *Proc. ICST BIONETICS 2008*, Hyogo, Japan, Nov. 2008, pp. 16:1–16:8.
- [10] M. J. Moore, T. Suda, and K. Oiwai, "Molecular communication: Modeling noise effects on information rate," *IEEE Trans. NanoBiosci.*, vol. 8, no. 2, pp. 169–179, June 2009.
- [11] Y. Okaie, T. Obuchi, T. Hara, and S. Nishio, "In silico experiments of mobile bionanosensor networks for target tracking," in *Proc. ACM NANOCOM 2015*, Boston, MA, Sept. 2015, pp. 14:1–14:6.
- [12] A. Einolghozati, M. Sardari, and F. Fekri, "Design and analysis of wireless communication systems using diffusion-based molecular communication among bacteria," *IEEE Trans. Wireless Commun.*, vol. 12, no. 12, pp. 6096–6105, Dec. 2013.
- [13] A. O. Bicen and I. F. Akyildiz, "Interference modeling and capacity analysis for microfluidic molecular communication channels," *IEEE Trans. Nanotechnol.*, vol. 14, no. 13, pp. 570–579, May 2015.
- [14] T. Nakano, Y. Okaie, and A. V. Vasilakos, "Transmission rate control for molecular communication among biological nanomachines," *IEEE J. Sel. Areas Commun.*, vol. 31, no. 12, pp. 835–846, Dec. 2013.
- [15] C. T. Chou, "Extended master equation models for molecular communication networks," *IEEE Trans. NanoBiosci.*, vol. 12, no. 2, pp. 79–92, June 2013.
- [16] B. H. Koo, C. Lee, H. B. Yilmaz, N. Farsad, A. Eckford, and C. B. Chae, "Molecular MIMO: From theory to prototype," *IEEE J. Sel. Areas Commun.*, vol. 34, no. 3, pp. 600–614, Mar. 2016.
- [17] I. Akyildiz, B. Lo, and R. Balakrishnan, "Cooperative spectrum sensing in cognitive radio networks: A survey," *Phys. Commun.*, vol. 4, no. 1, pp. 40–62, Mar. 2011.
- [18] P. K. Varshney, *Distributed Detection and Data Fusion*. New York, NY: Springer-Verlag, 1997.
- [19] A. P. de Silva and S. Uchiyama, "Molecular logic and computing," *Nature Nanotech.*, vol. 2, no. 7, pp. 399–410, July 2007.
- [20] U. Pischel, "Chemical approaches to molecular logic elements for addition and subtraction," *Angew. Chem. Int. Ed.*, vol. 46, no. 22, pp. 4026–4040, 2007.
- [21] J. N. Laneman, D. N. C. Tse, and G. W. Wornell, "Cooperative diversity in wireless networks: Efficient protocols and outage behavior," *IEEE Trans. Inf. Theory*, vol. 50, no. 12, pp. 3062–3080, Nov. 2004.

- [22] A. Ahmadzadeh, A. Noel, and R. Schober, "Analysis and design of multi-hop diffusion-based molecular communication networks," *IEEE Trans. Mol. Biol. Multi-Scale Commun.*, vol. 1, no. 2, pp. 144–157, June 2015.
- [23] M. S. Kuran, H. B. Yilmaz, T. Tugcu and I. F. Akyildiz, "Modulation techniques for communication via diffusion in nanonetworks," in *Proc. IEEE ICC 2011*, Kyoto, Japan, June 2011, pp. 1-5.
- [24] A. Noel, K. C. Cheung, and R. Schober, "Optimal receiver design for diffusive molecular communication with flow and additive noise," *IEEE Trans. NanoBiosci.*, vol. 13, no. 3, pp. 350–362, Sept. 2014.
- [25] A. Noel, K. C. Cheung, and R. Schober, "Using dimensional analysis to assess scalability and accuracy in molecular communication," in *Proc. IEEE ICC 2013 MoNaCOM Workshop*, Budapest, Hungary, June 2013, pp. 818–823.
- [26] S. Boyd and L. Vandenberghe, *Convex Optimization*. Cambridge University Press, 2004.
- [27] R. Horn and C. Johnson, *Matrix Analysis*. Cambridge University Press, 1985.